Effects of 3D Magnetic Field Structure to MHD Equilibrium and Stability

- aspects from Stellarator/Heliotron Researches

Yasuhiro Suzuki

for the LHD team

National Institute for Fusion Science
The Graduate University for Advanced Studies SOKENDAI
Toki, Japan
suzuki.yasuhiro@LHD.nifs.ac.jp

Special thanks to S.Sakakibara, K.Y.Watanabe, S.Ohdachi, K.Ida, N.Mizuguchi, Y.Todo, H. Yamada

LHD NIFS

NINS
National Institutes of Natural Sciences

4th International ITER Summer School
Austin 31 May - 4 June, 2010

Outline

1. What is Stellarator?
2. The Large Helical Device – LHD -
3. MHD Equilibrium in 3D Field
4. Interaction of the instability and 3D Field
5. Application of 3D tools to Tokamak
6. Summary

1. What is Stellarator?

Another candidate for Fusion Reactor

Why is the rotational transform necessary?

For simple torus…

Charge separation appears by grad-*B* drift.

⇓

Electric field is driven.

⇓

Disruption!

To cancel the charge separation, the connection between up and down of the plasma is necessary. => twist the field lines.

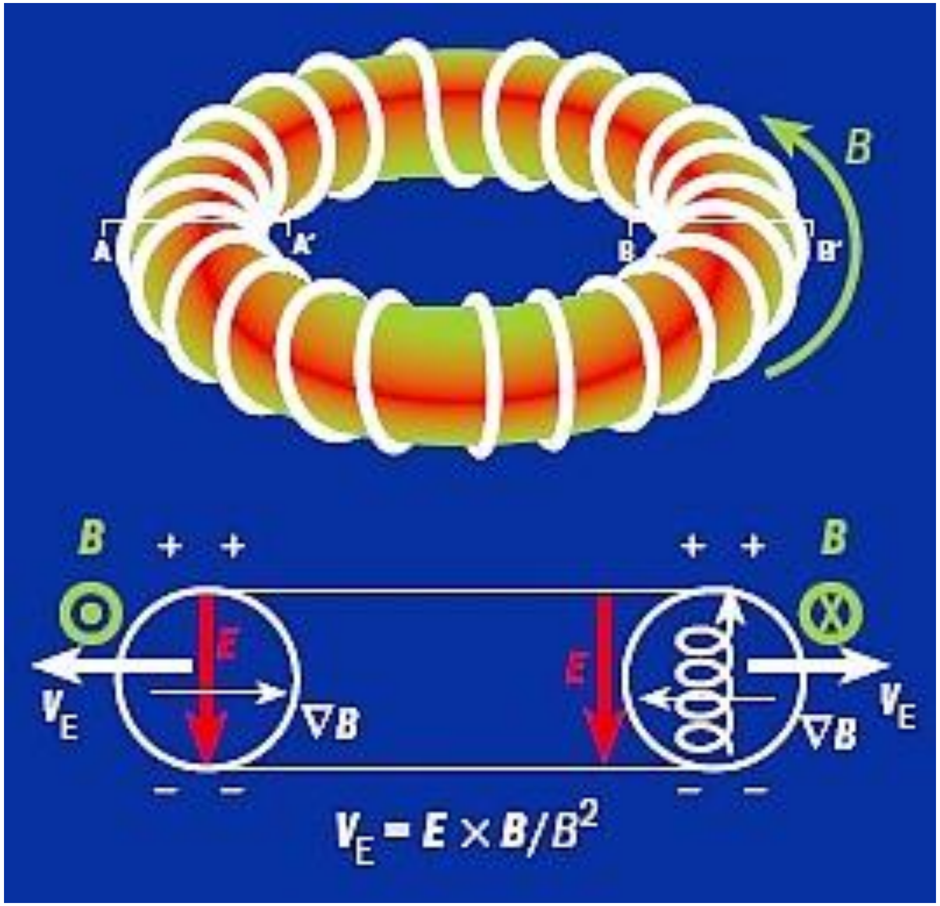

http://www.scidacreview.org/0801/html/fusion1.html

Classification of the rotational transform creating

C.Mercier, “Lectures in Plasma Physics”

- Toroidal current along the axis => tokamaks
- Torsion of the axis => 8-figure stellarator
- Modulation of flux surfaces

L.Spizter Jr.

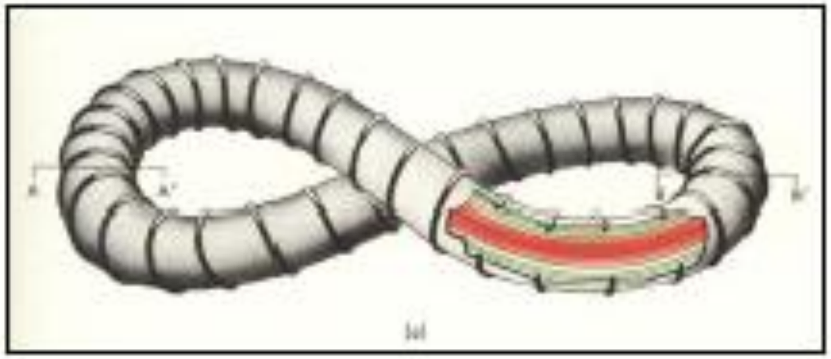

Model A stellarator, 1951, Princeton

Classification of the rotational transform creating

C.Mercier, "Lectures in Plasma Physics"

- Toroidal current along the axis
- Torsion of the axis
- Modulation of flux surfaces

Stellarators create the rotational transform by 3D shaping.

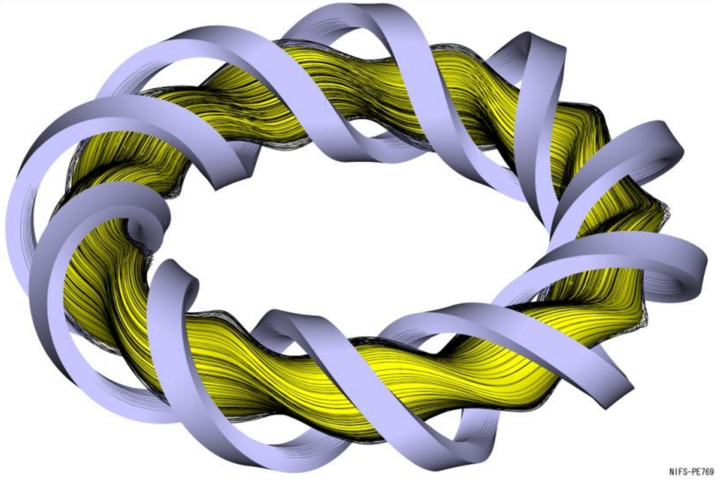

Advantages:

1. **Steady-state operation without current drive**
2. **No disruptin**

Classification of the rotational transform creating

C.Mercier, “Lectures in Plasma Physics”

- Toroidal current along the axis
- Torsion of the axis
- Modulation of flux surfaces

Stellarators create the rotational transform by 3D shaping.

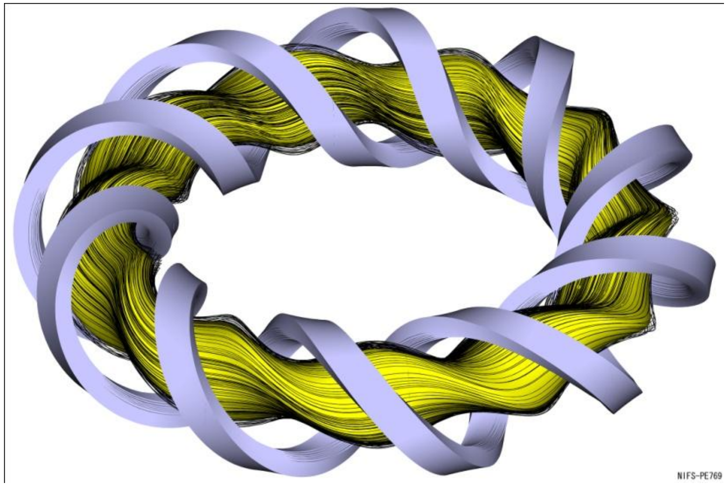

Disadvantages:

1. **Engineering problems**
2. **Degradation of the confinement by helical ripples**

Model C Stellarator "Race Track"

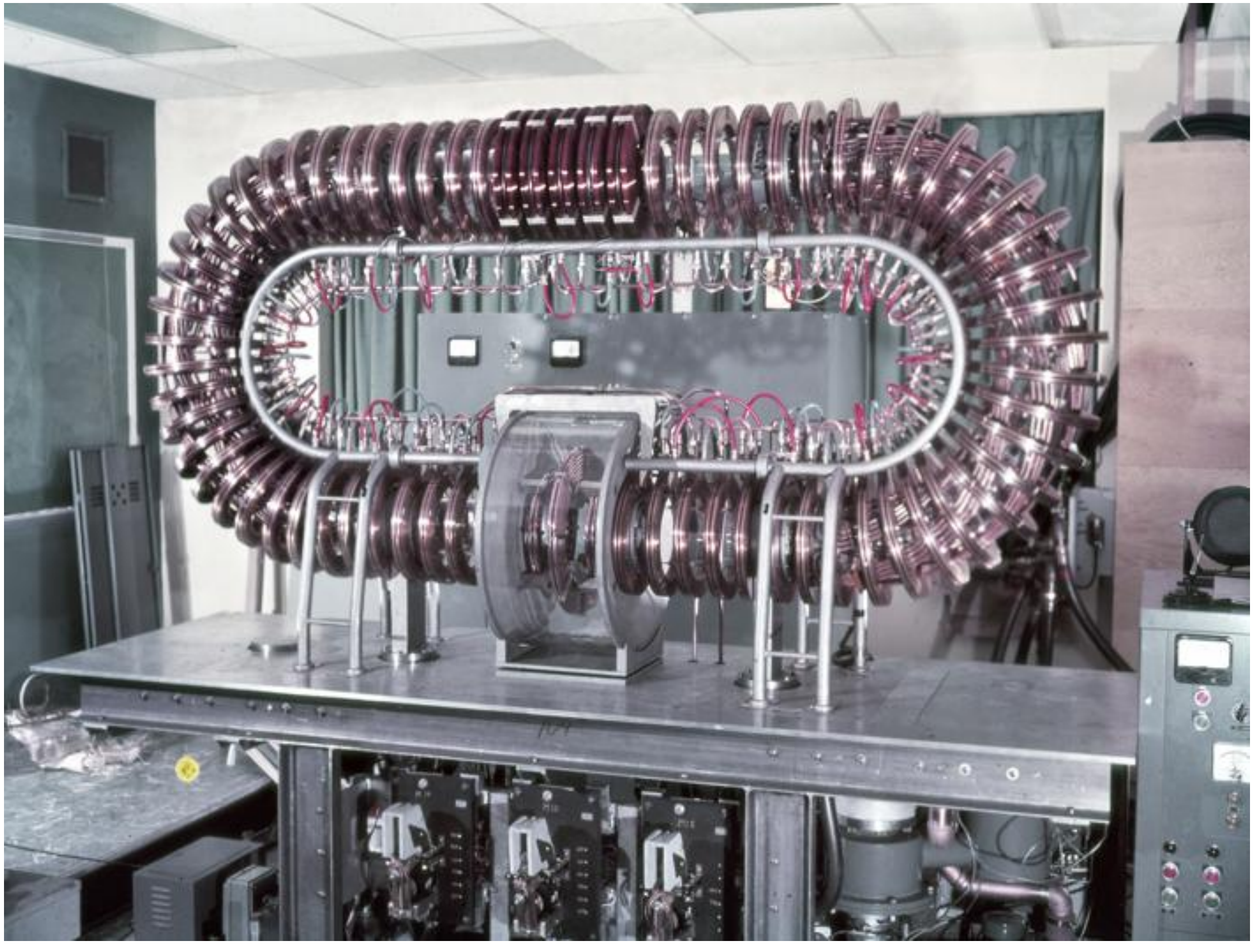

Courtesy to PPPL

Helical-axis Stellarator "Asperator"

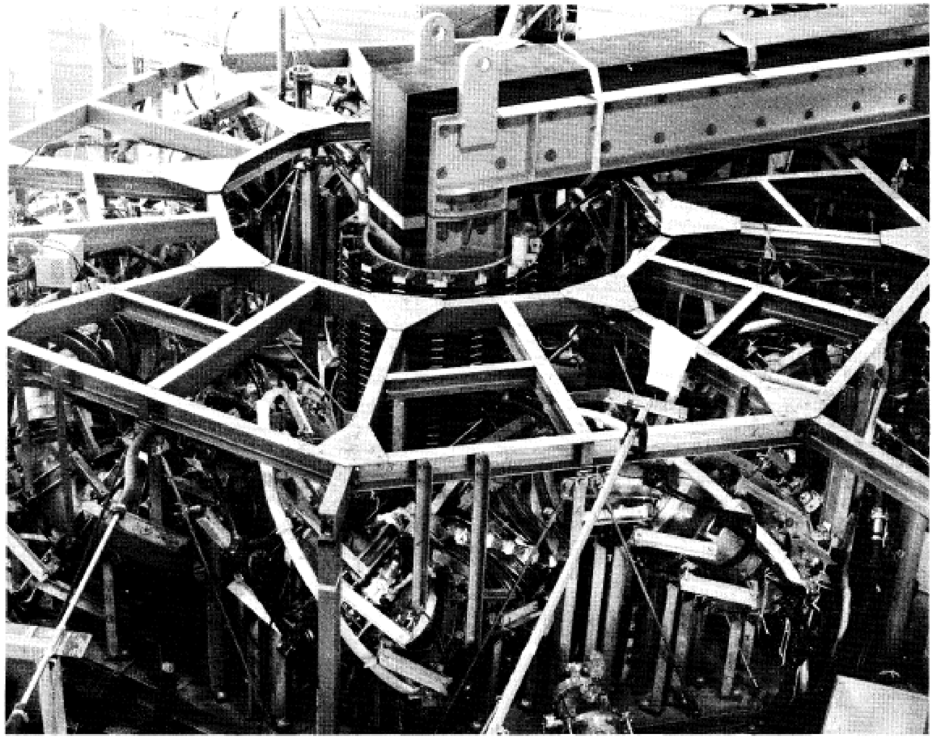

Fig. 1. Asperator NP-4.

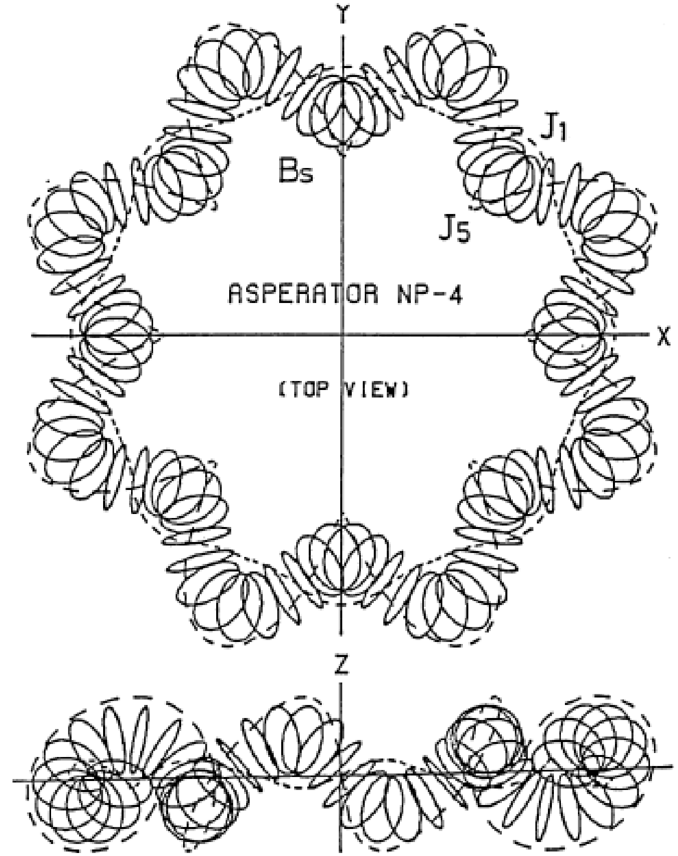

Y.Funato, *et al*., Japanese Journal of Applied Physics **22** (1983) 1188
Y.Funato, *et al*., Japanese Journal of Applied Physics **27** (1988) 821

LHD has worked very well for 10 years

Courtesy to H.Yamada SOFT2008

- ✓ Construction completed within the eight-year plan (FY1990-1997)
- ✓ **Operation for 10 years**
- ➔ engineering base of a large-scale superconducting and cryogenic system for a fusion reactor

< LHD basic dimension >

• Outer diameter	13.5 m
• Cold mass	820 ton
• Total weight	1500 ton
• Magnetic field	3 T
• Magnetic energy	0.77 GJ

Several-month-long operation, 11 times since 1998

- Operational time of He compressor : 51,654 hours
  ➔ Duty = 99.3 %
- Coil excitation number : 1,168 times
- Plasma discharges : 84,869 shots

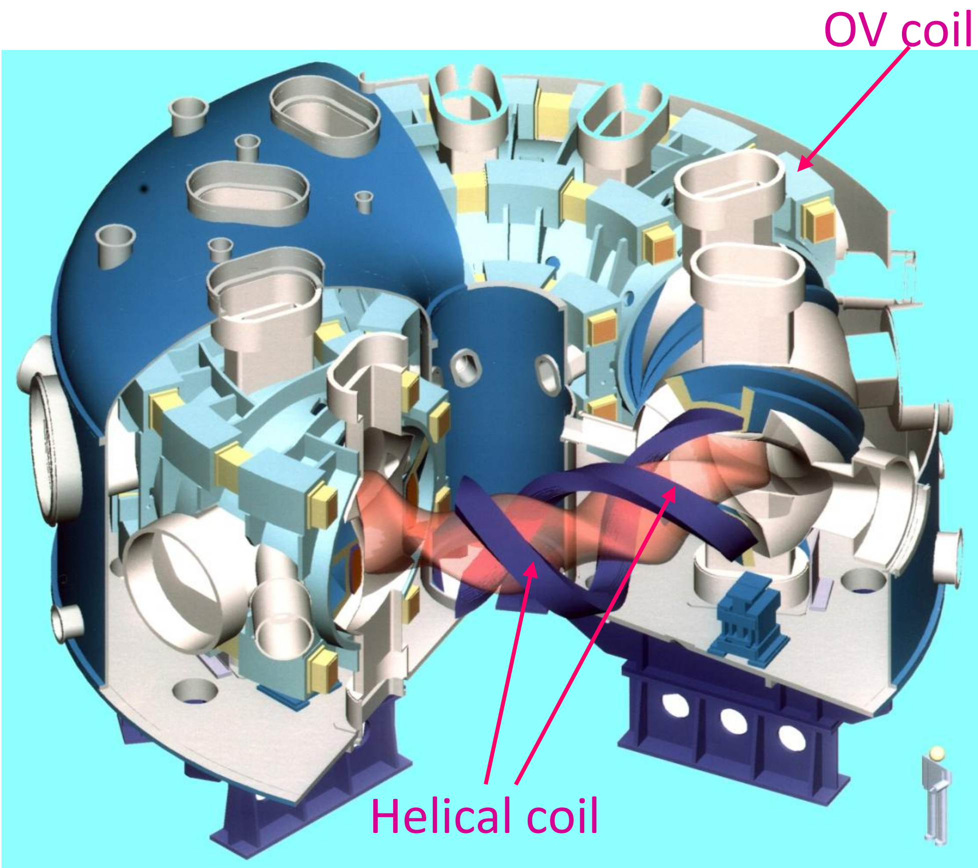

Stellarators have “vacuum flux surfaces”

Vacuum flux surfaces in a heliotron configuration

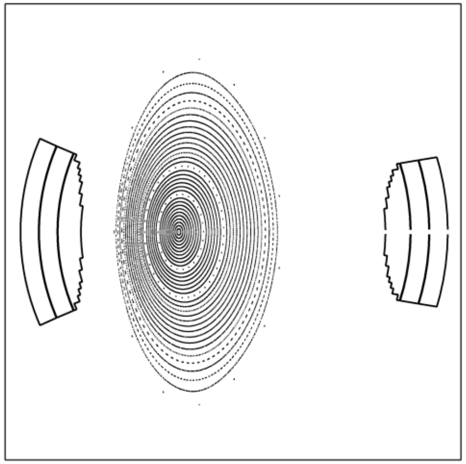
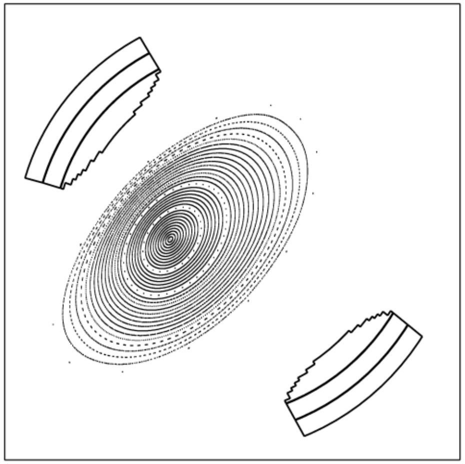
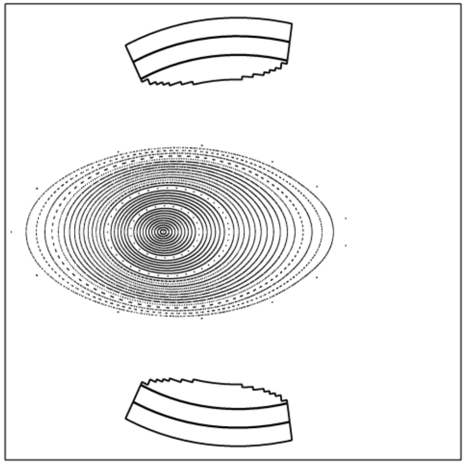
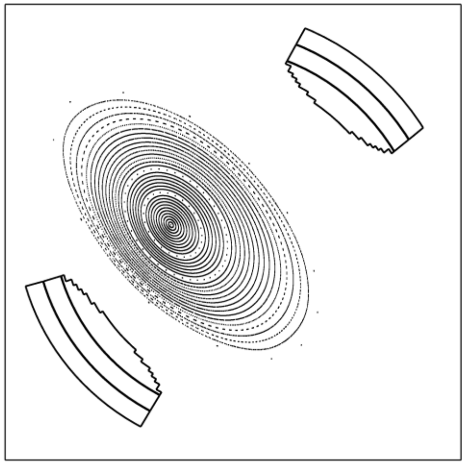
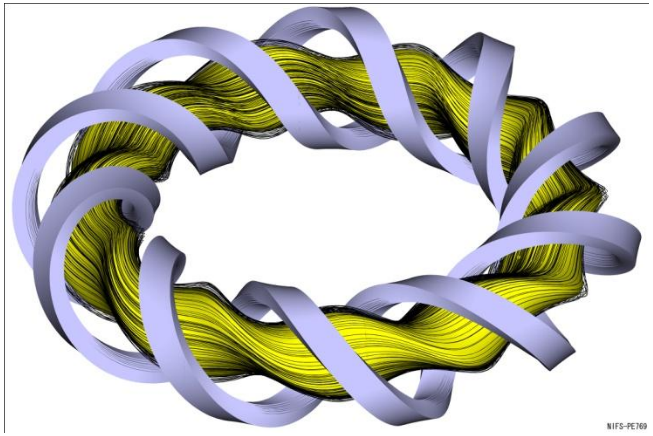

Stellarator field has toroidal periodicity.

Flux surfaces are changed due to the “plasma response”

3D MHD equilibrium analysis of an LHD plasma

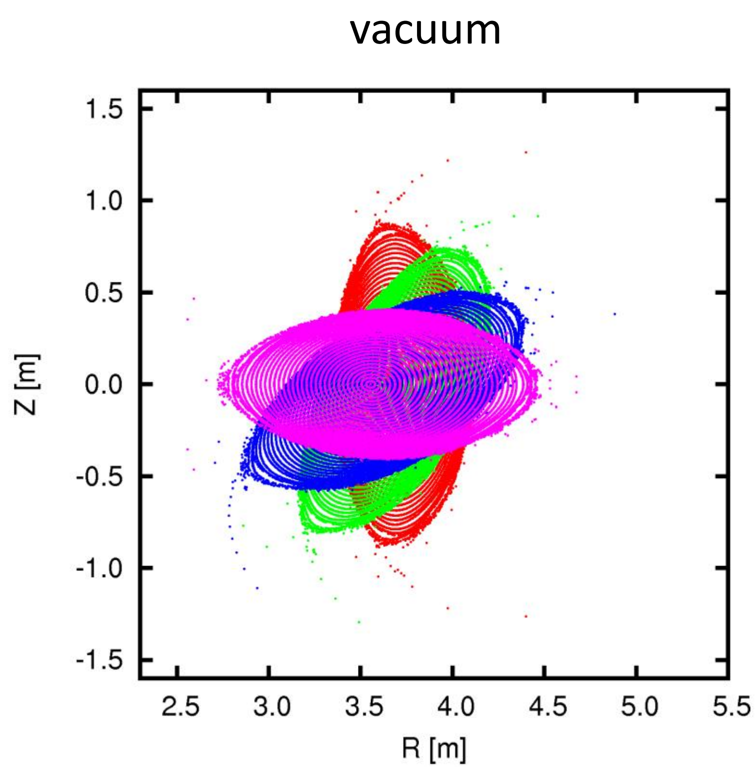

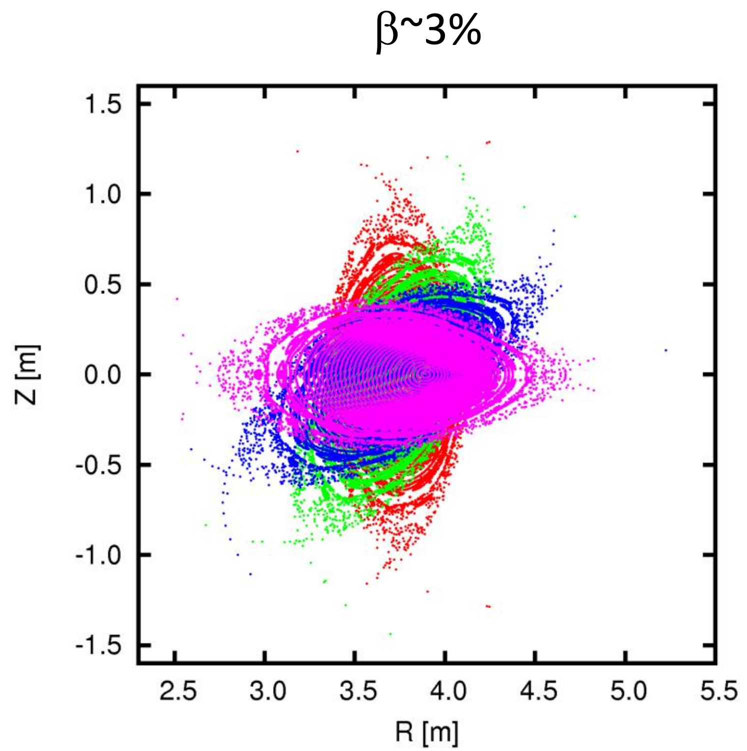

However, the plasma response strongly depend on the vacuum configuration!

Stellarator is not disruptive

Collapsed events are observed but not disruptive!

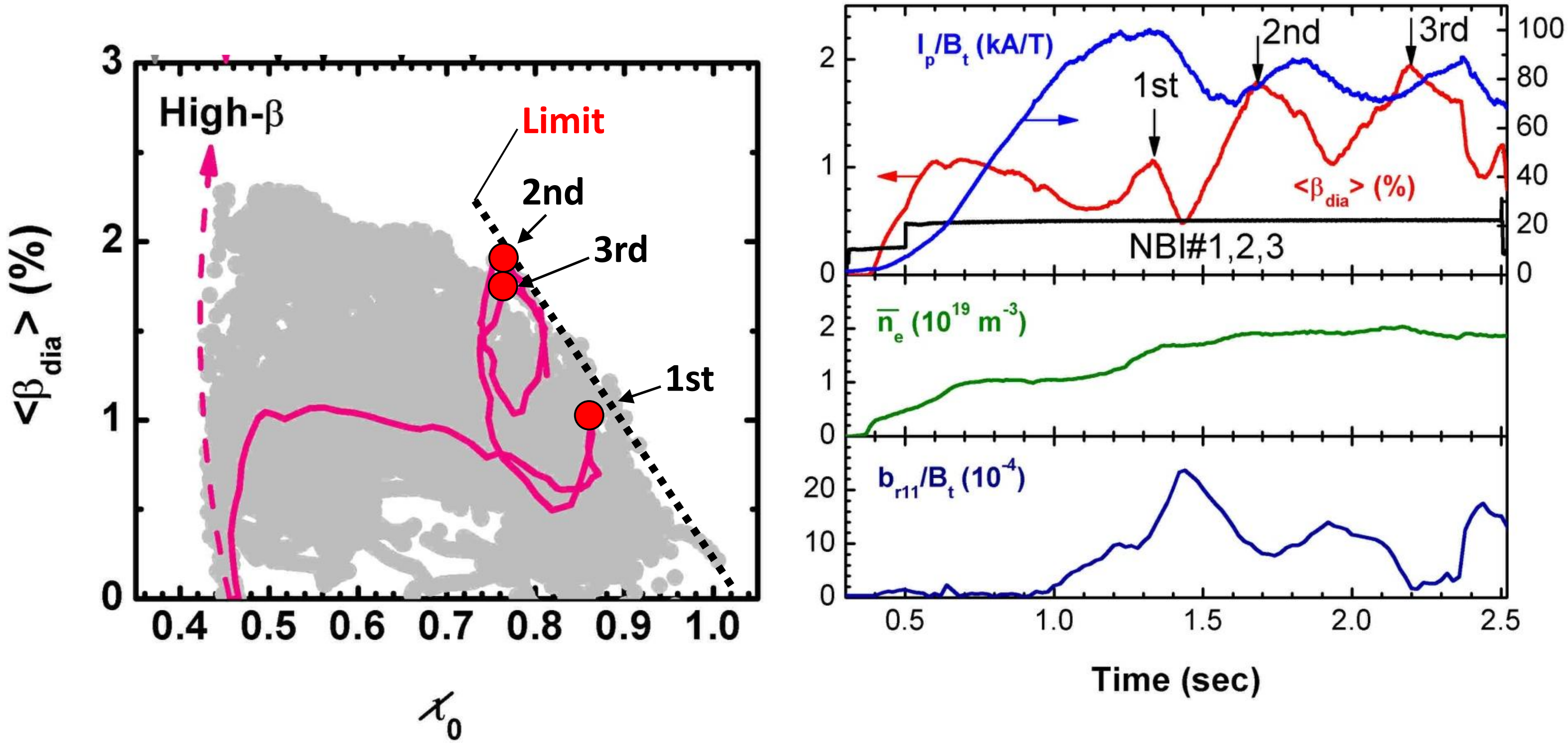

Plasma recovered after events!

What is the contribution from the stellarator research to ITER?

In tokamaks, the magnetic field to confine the plasma is produced by the plasma itself!

$$B_{\text{total}} = B_{\text{tor,vac}} + B_{\text{pol,plasma}} + B_{\text{response}}$$

$$\Updownarrow$$

In stellarators, the magnetic field to confine the plasma is produced by external coils for the vacuum.

$$B_{\text{total}} = B_{\text{tor,vac}} + B_{\text{pol,vac}} + B_{\text{response}}$$

$$\Downarrow$$

$$B_{\text{response}} = B_{\text{total}} - B_{\text{tor,vac}} - B_{\text{pol,vac}}$$

Stellarators are platforms to explorer 3D physics!

2. The Large Helical Device (LHD)

Present View! Large Helical Device (LHD)

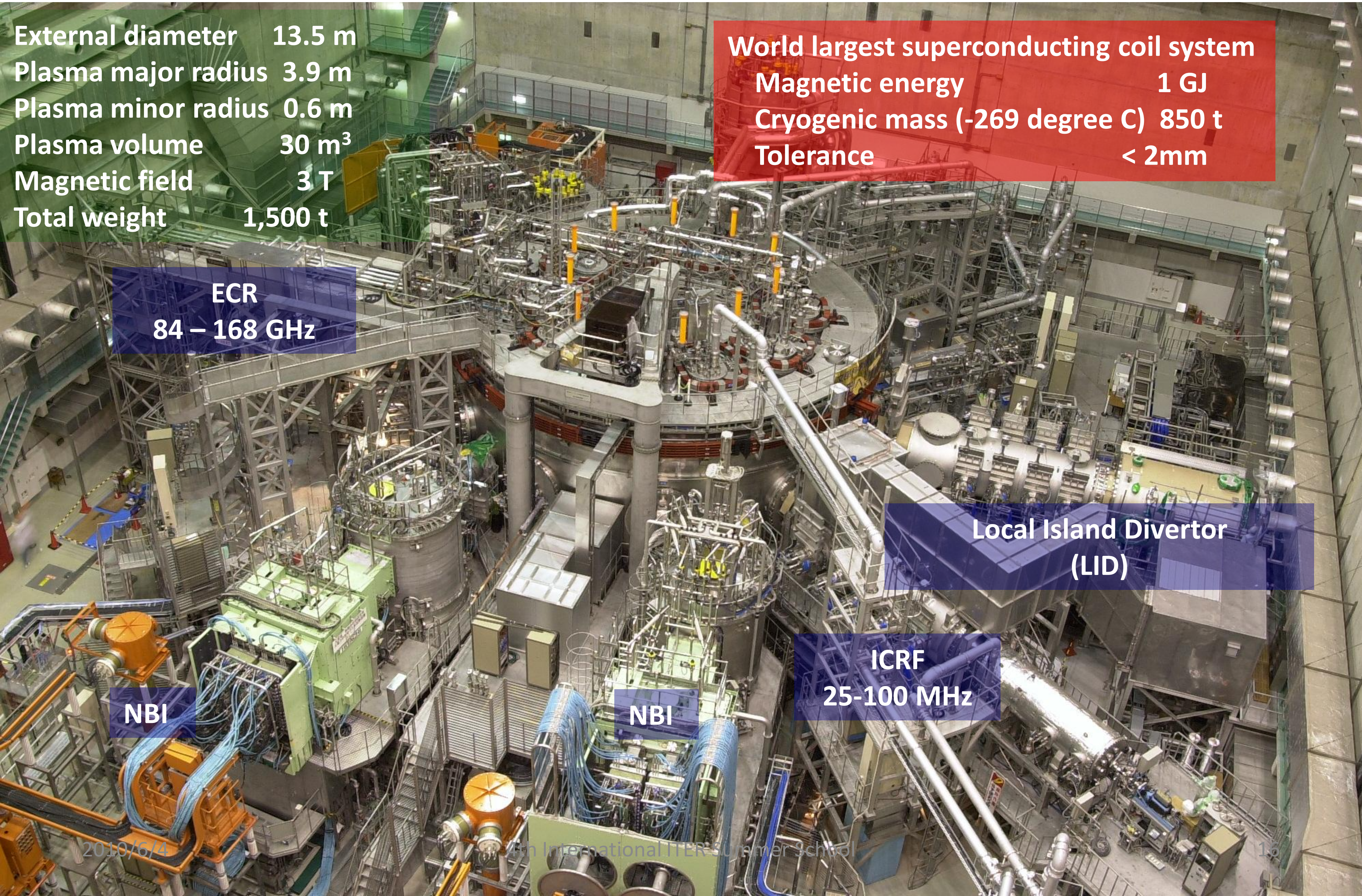

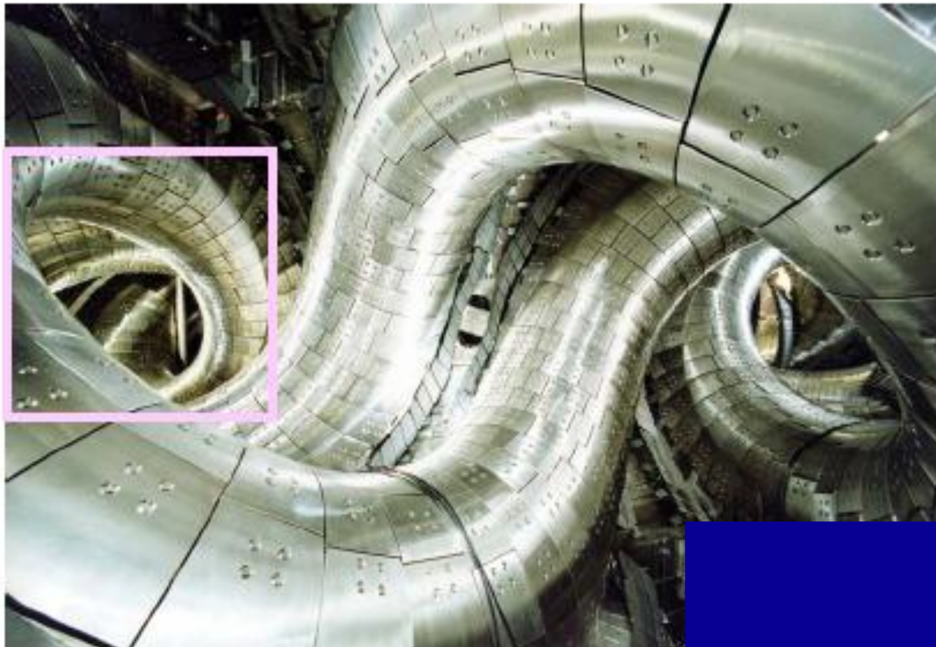

LHD

R = 3.9 m
a = 0.6 m
B = 3 T
P_{heat} = 20 MW

Superconducting coils with magnetic energy of 0.9GJ

80sec Discharge

LHD has large flexibility of magnetic configuration

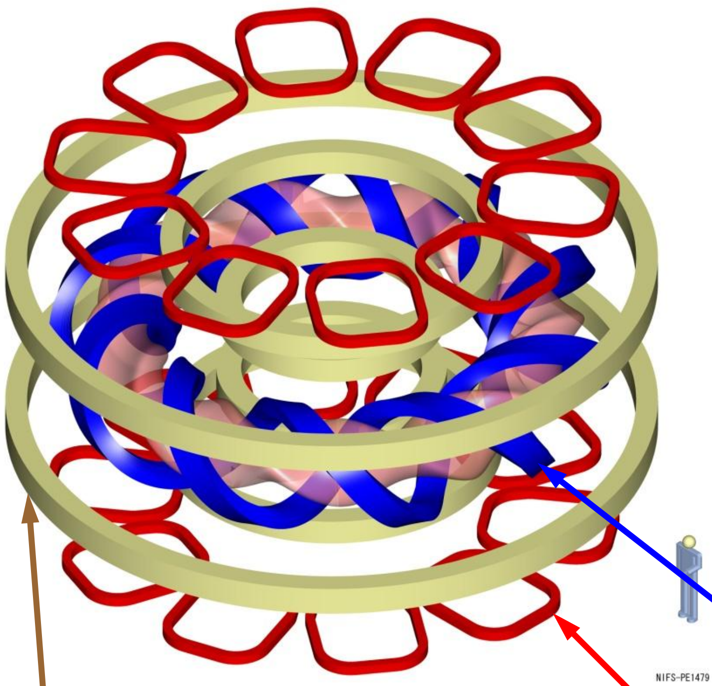

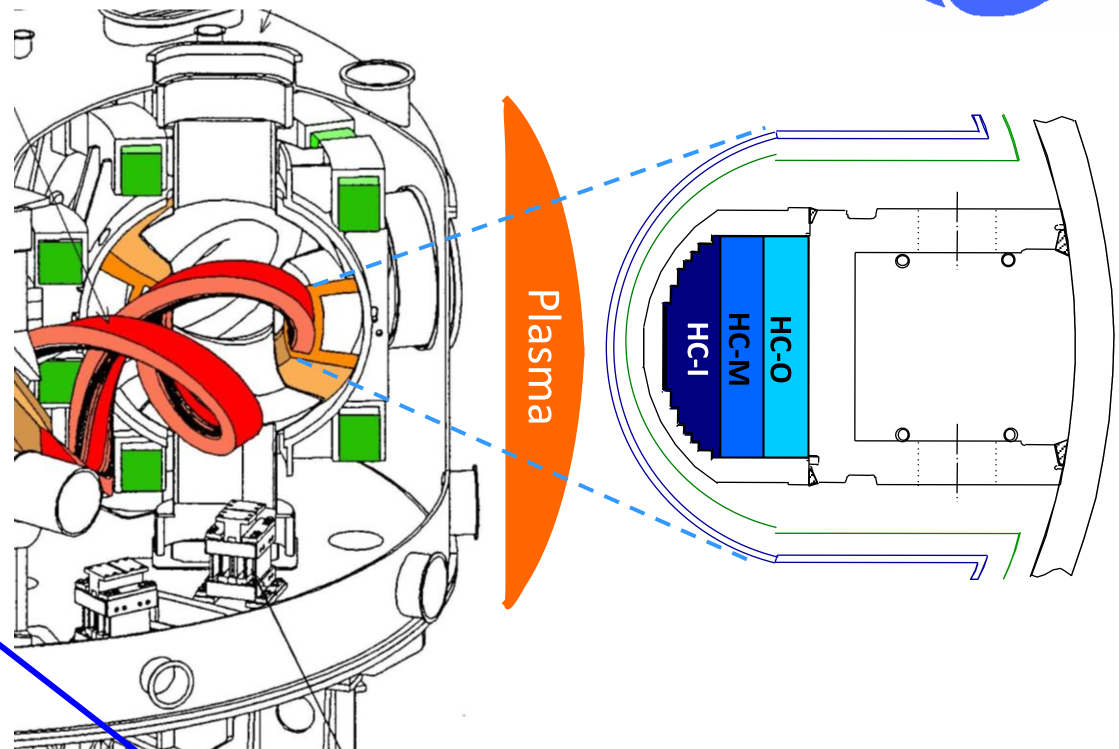

Poloidal field coil

➔ Position of magnetic axis

➔ Elongation

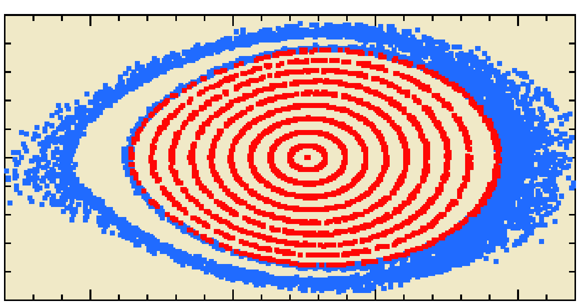

Control of current center of helical coil

➔ Aspect ratio

➔ Rotational transform

Local Island Divertor coil

➔ Generates m/n=1/1 Resonant Magnetic Perturbation (RMP)

➔ Magnetic island

Typical Iota profile and well/Hill boundary

- In LHD, pressure gradient driven modes are important; stability depends on magnetic well depth.
- With increase of beta, the well region expands.
- Unstable region remains in the edge region.
- Resistive interchange mode always observed in the edge. (slightly increase transports)

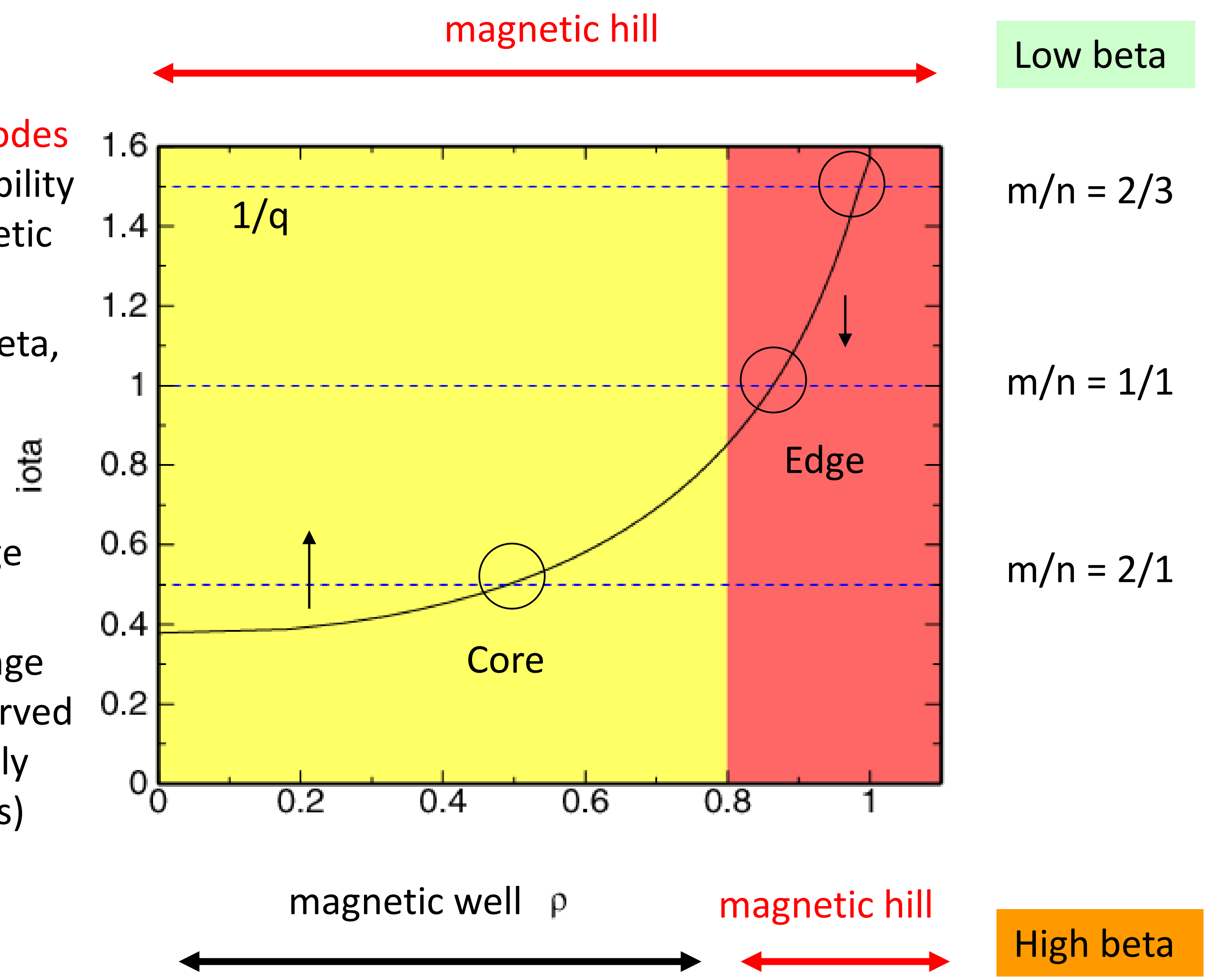

Magnetic well is created due to the Shafranov shift

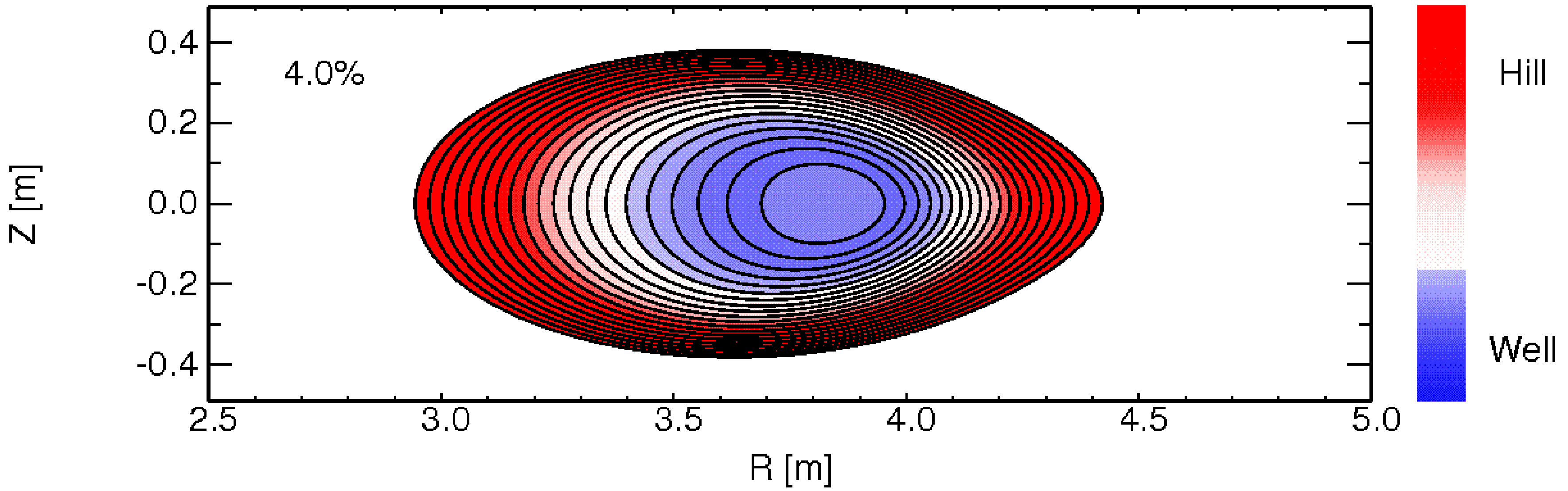

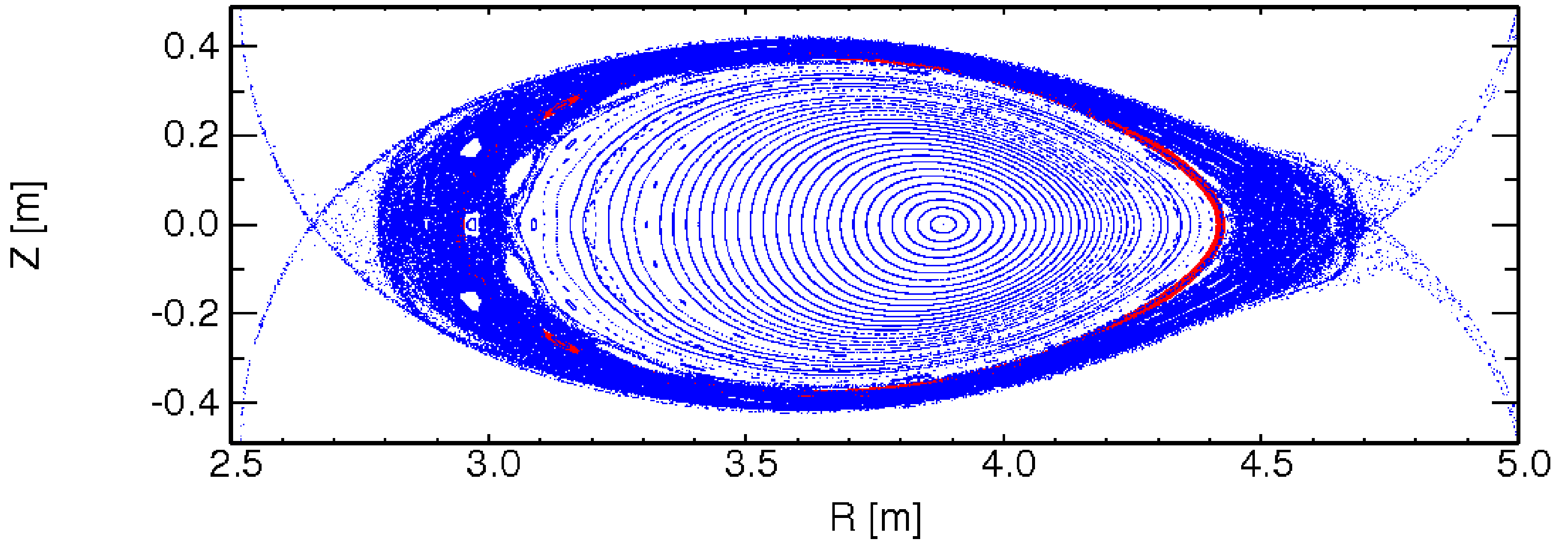

Subjects of MHD studies in Heliotron

MHD equilibrium, **stability** and **transport** are key issues for production of high-beta plasmas:

MHD Equilibrium:

- Change of magnetic topology and relationship with beta-limit

  - Stochastization of peripheral magnetic field lines

MHD Stability:

- Effect of pressure-driven mode (Interchange and Ballooning modes)

  - Magnetic hill in the periphery

Transport:

- transport related with finite-*b* effects (magnetic topology, beta and so on)

  - Particle loss due to an increment of helical ripple, turbulence caused by steep ∇p

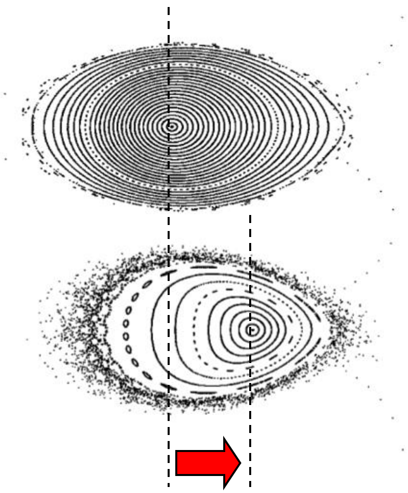

<*b*> ~ 0 %

<*b*> ~ 4 %

3 . 3D MHD Equilibrium studies

3.1 Stochastization due to plasma response

High-beta Steady State Discharge

- $\langle\beta\rangle_{max}$ ~ 4.8 %, β_0 ~ 9.6 %, H_{ISS95} ~ 1.1
- Plasma was maintained for $85\tau_E$
- Shafranov shift Δ/a_{eff} ~ 0.25
- Peripheral MHD modes are dominantly observed.

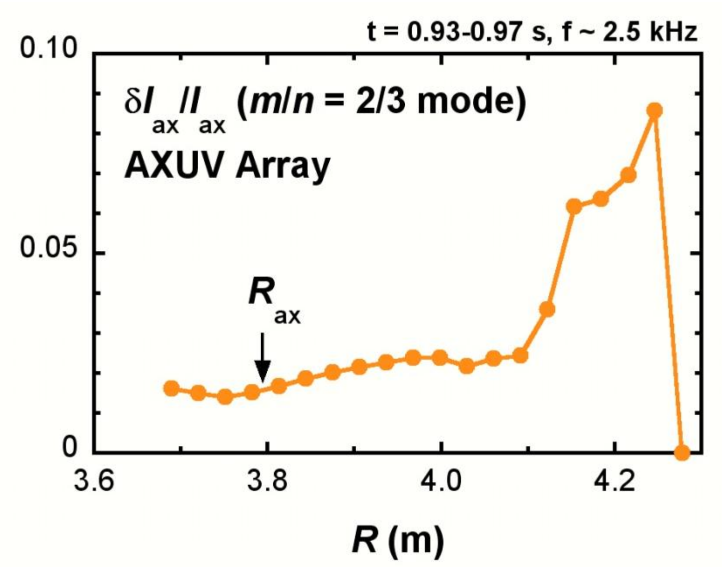

R_{ax} = 3.6 m, B_t = -0.425 T

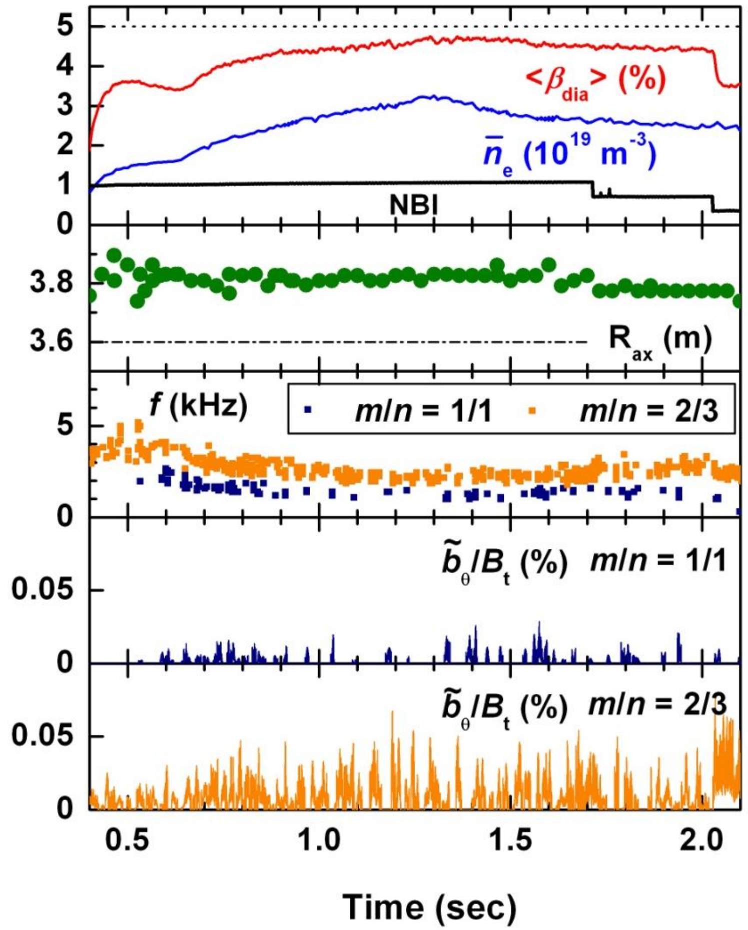

High-beta Discharge – Pellet Injection –

▶ Perpendicular-NBI was applied after several pellets were injected and tangential NBI is turned off which leads to reduction of Shafranov shift.

▶ MHD activity is not enhanced in high-beta regime with more than 4 %

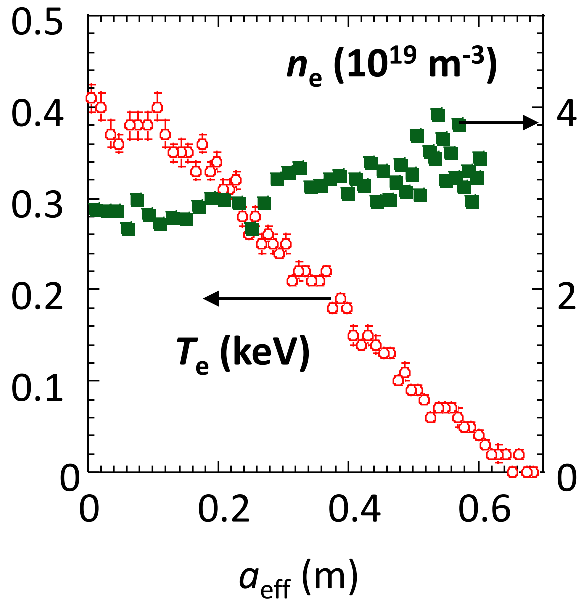

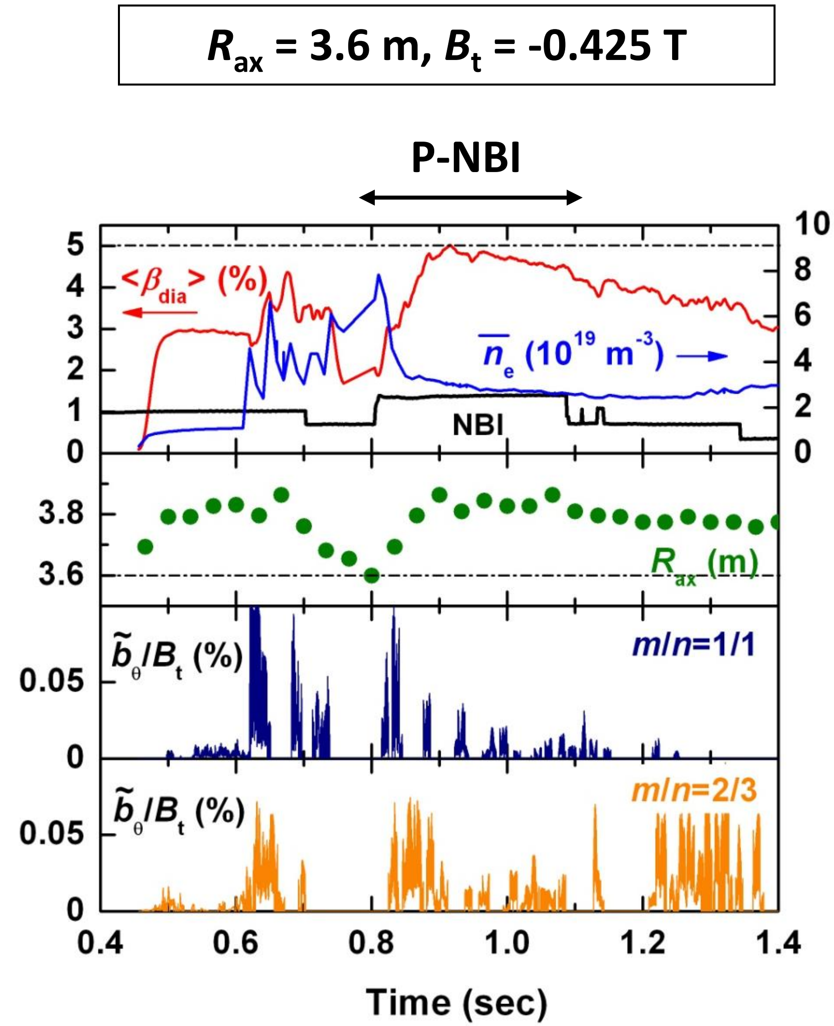

Achievement of the High beta plasma in LHD

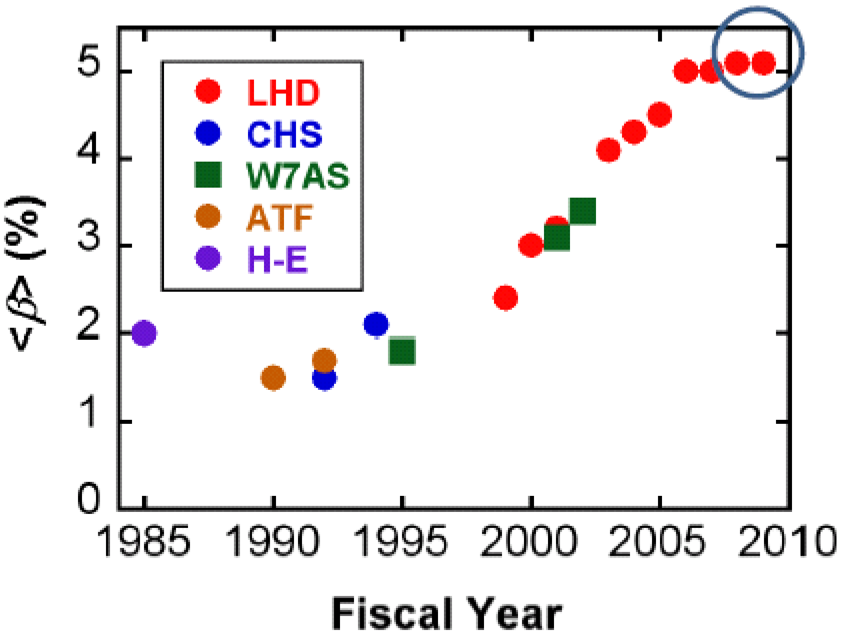

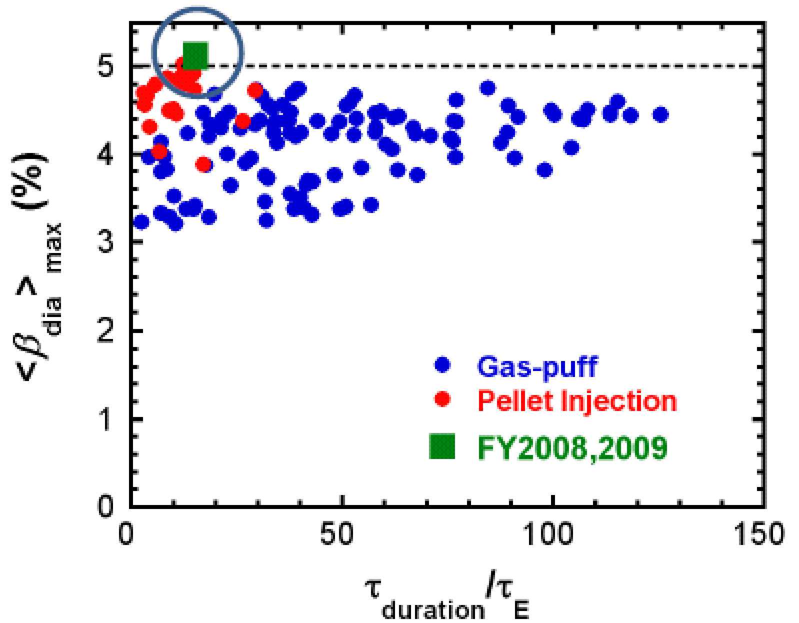

Sustainment of the high-beta plasma is not a serious problem in helical system($\tau_{duration}/\tau_E > 100$). Limited only by the heating source.

Question: How far is from the beta limit?

How about is the magnetic surface topology?

Degradation of flux surfaces due to increasing β

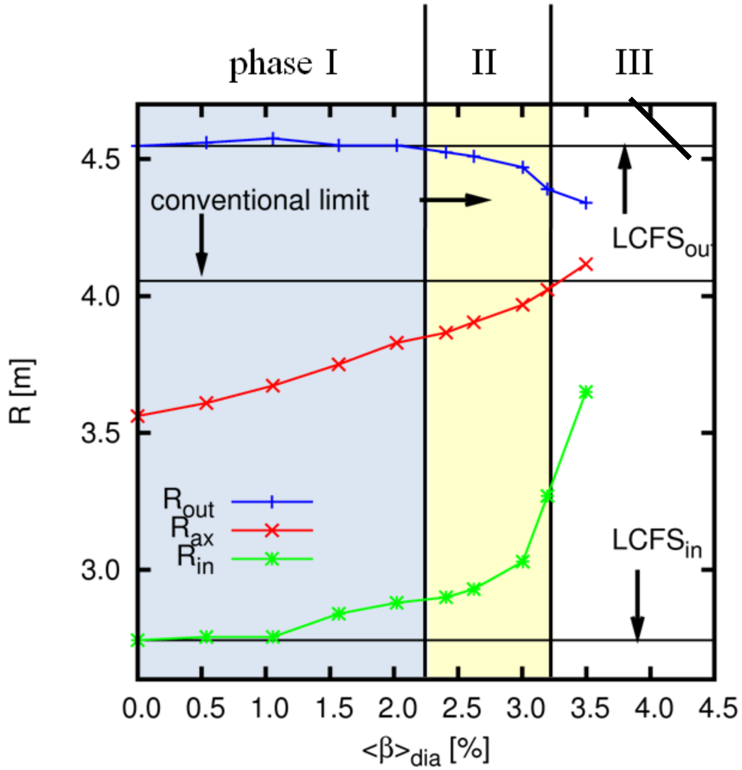

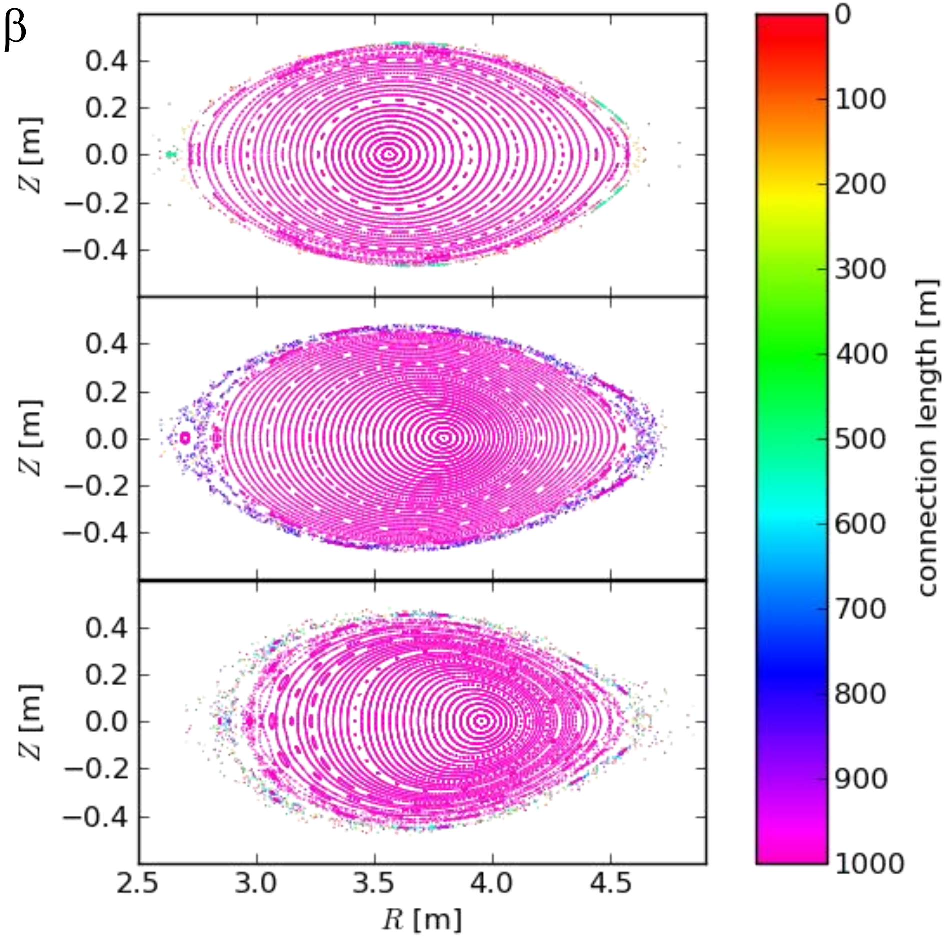

In the peripheral region, magnetic field lines become stochastic as b increases.
The volume inside LCFS shrinks drastically.

Control Coil Variation Changes Flux Surface Topology

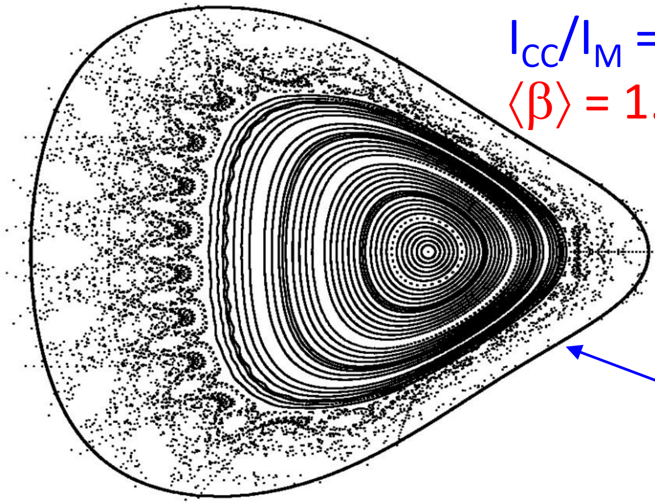

$I_{CC}/I_M = 0$
$\langle\beta\rangle = 1.8\%$

VMEC boundary

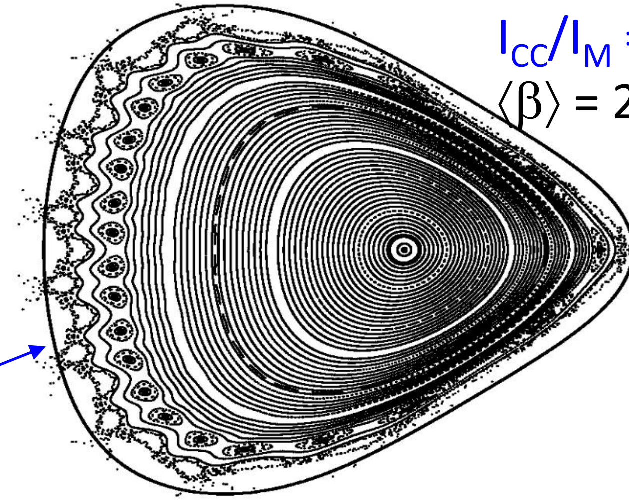

$I_{CC}/I_M = 0.15$
$\langle\beta\rangle = 2.0\%$

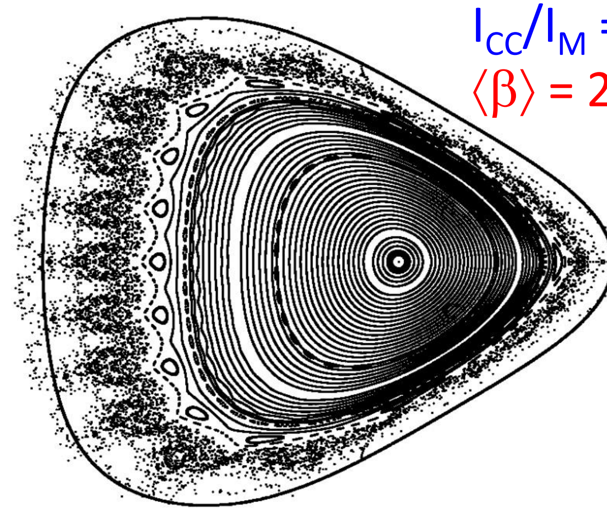

$I_{CC}/I_M = 0.15$
$\langle\beta\rangle = 2.7\%$

- PIES equilibrium analysis using fixed pressure profile from equilibrium fit (not yet including current profile).

- Calculation: at ~ fixed β, I_{CC}/I_M=0.15 gives better flux surfaces

- At experimental maximum b values
  -- 1.8% for I_{CC}/I_M =0
  -- 2.7% for I_{CC}/I_M = 0.15
  calculate similar flux surface degradation

Courtesy to M.C.Zarnstorff and A.H. Reiman

Edge T_e does not respond to P_{inj}

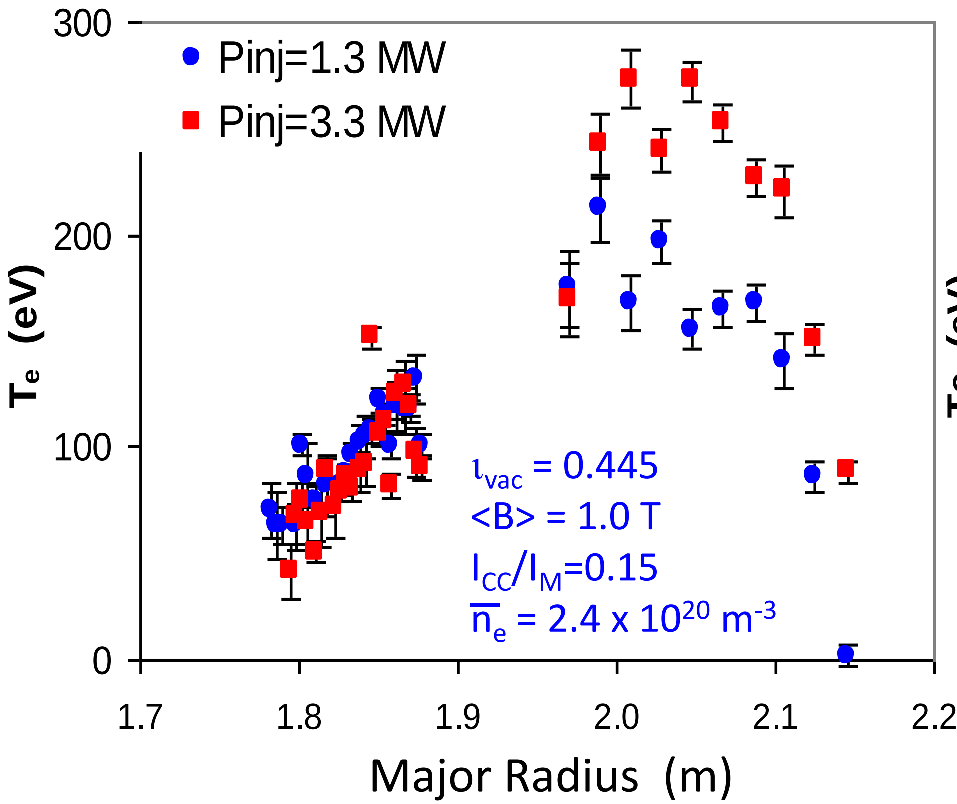

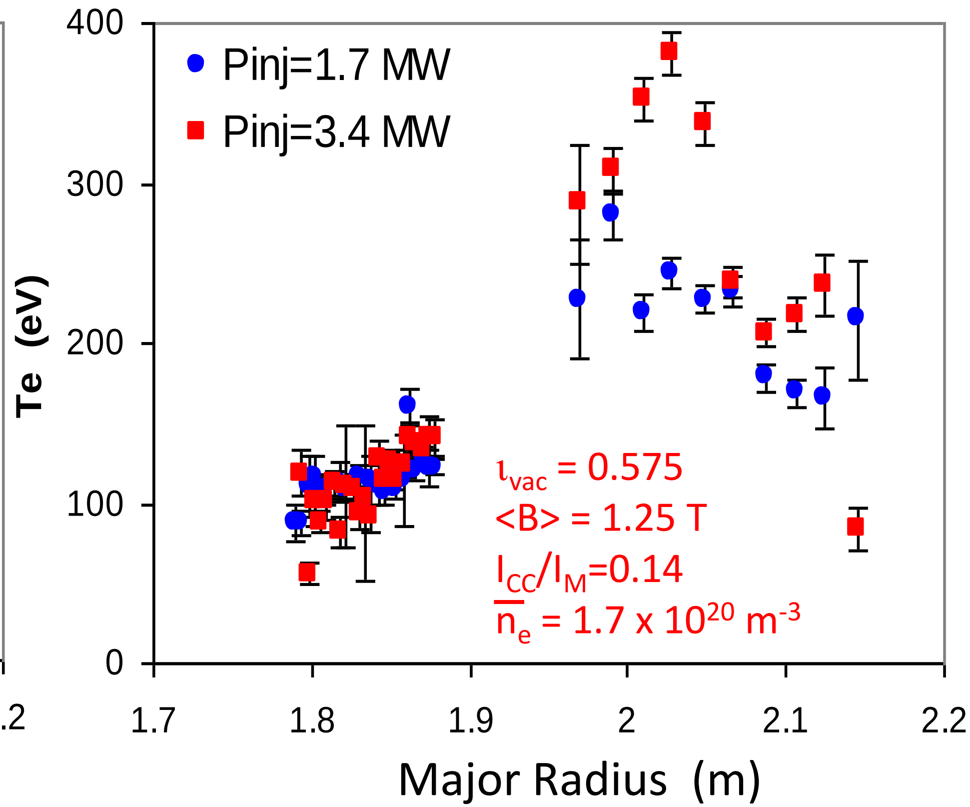

- Edge T_e and ∇T_e does not change with increasing P_{inj} !!
  $\Rightarrow$ Radial transport degrading as power increases
- Fixed density, and constant n_e profile. Increase in β due to core T_e increase
- Edge ∇T_e lower for ι = 0.575 $\Rightarrow$ higher radial transport.

Courtesy to M.C.Zarnstorff and A.H. Reiman

Results from HINT well describes deformation of magnetic surfaces

3-D equilibrium consistent with experimental observation, i.e., Shafranov shift, pressure profile, etc.

Significant pressure (T_e) gradient exists in the edge stochastic area

Hypothesis

1) Plasma heals flux surfaces
2) Profile is consistent with characteristics of stochastic field
3) Somewhere between 1) & 2)

$L_{C\text{-}TB}$: connection length between the torus-top and - bottom

✓ L_C >> $L_{C\text{-}TB}$

➔ Pfirsch-Schlüter current is effective

➔ Secure MHD equilibrium

✓ L_C >> **MFP** (even under a reactor condition)

➔ Plasma is collisional enough to secure isotropic pressure

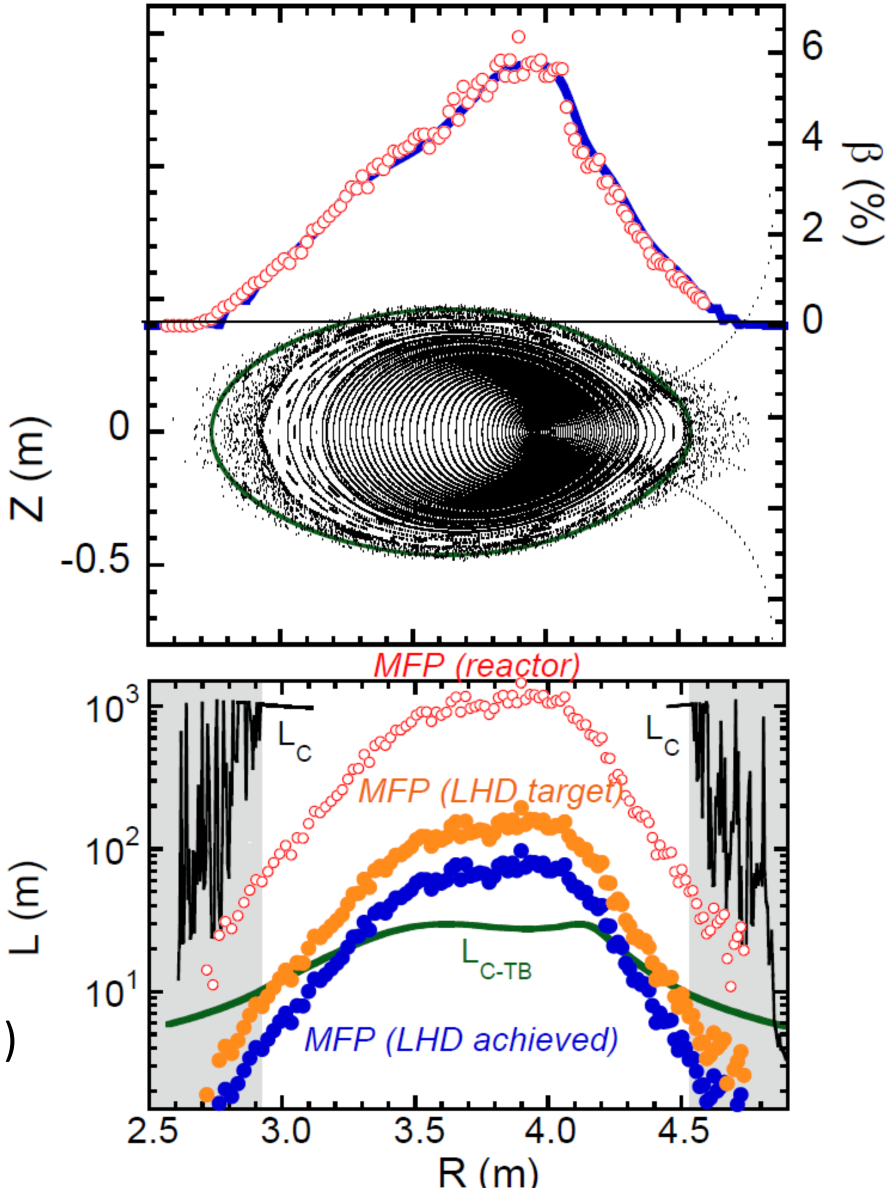

How large is the stochasticity?

Degradation of surface quality due to β

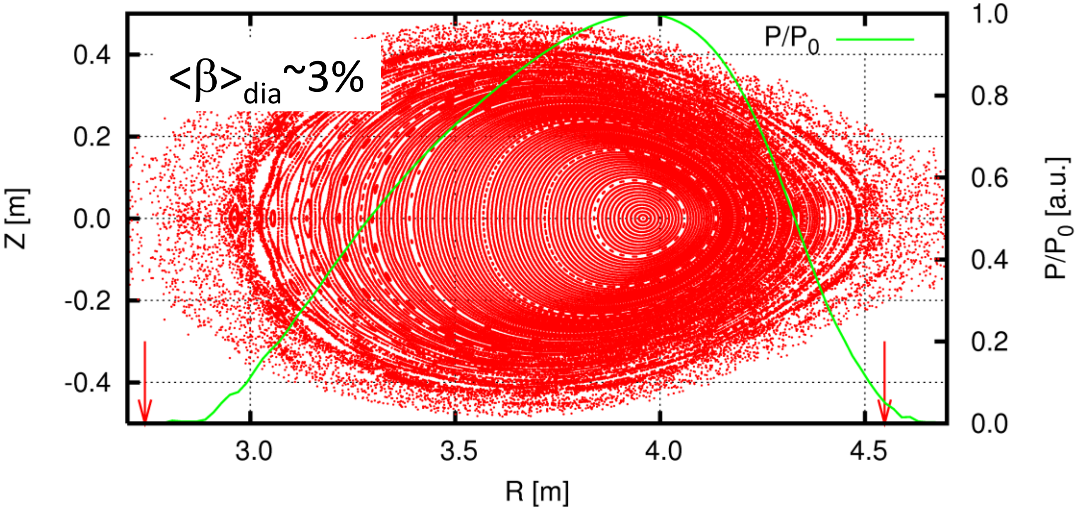

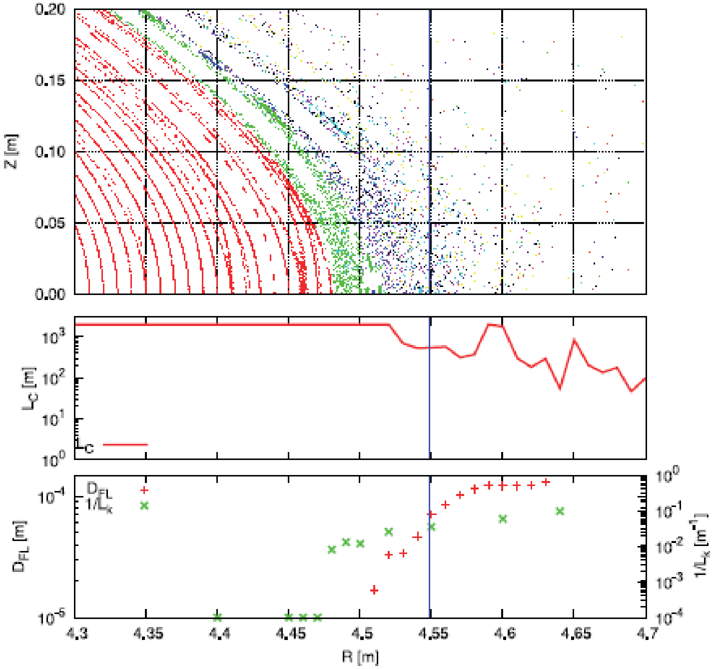

- Two arrows indicate the position of well-defined LCFS on the equatorial plane.
- Flux surfaces in the peripheral region degrade due to the increased β.
- The plasma pressure exists in the stochastic region.

In collisional plasmas(λ_e<L_k<L_C), radial heat diffusivity is defined by,

$$\chi_r = D_{FL}\chi_{\parallel} / L_k$$

This formula means parallel diffusion is effective as well as perpendicular diffusion.

3 . 3D MHD Equilibrium studies

3.2 3D MHD Equilibrium with magnetic island

Magnetic shear control experiments

Resonant magnetic field

- LHD has the compensation coil system to cancel out the error field and to perform advanced divertor scenario (LID)
- Dominant Fourier component is m/n = 1/1.
- Negative coil current can cancel out the natural error field with m/n = 1/1.

$I_{\mathrm{LID}}/B_{\mathrm{t}} < 0$

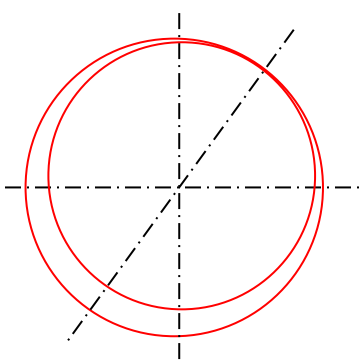

O-point (f = -126°)

$I_{\mathrm{LID}}/B_{\mathrm{t}} > 0$

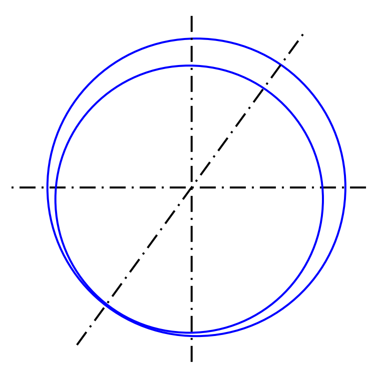

O-point (f = 54°)

Natural island : f = -90° ~ -126°

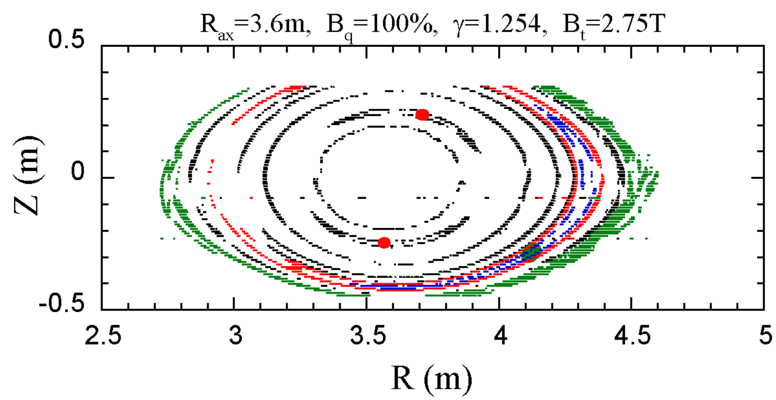

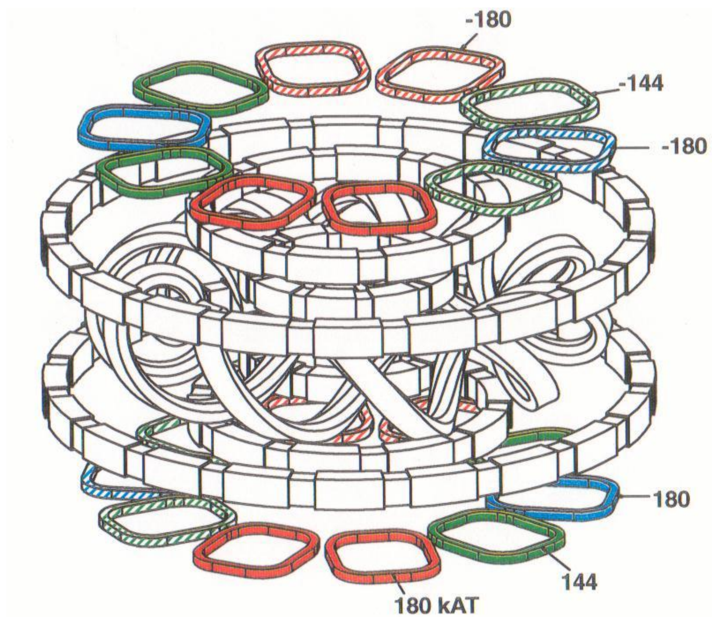

Intrinsic islands

- LHD has the compensation coil system to cancel out the error field and to perform advanced divertor scenario (LID)
- Dominant Fourier component is m/n = 1/1.
- Negative coil current can cancel out the natural error field with m/n = 1/1.

Natural island : f = -90° ~ -126°

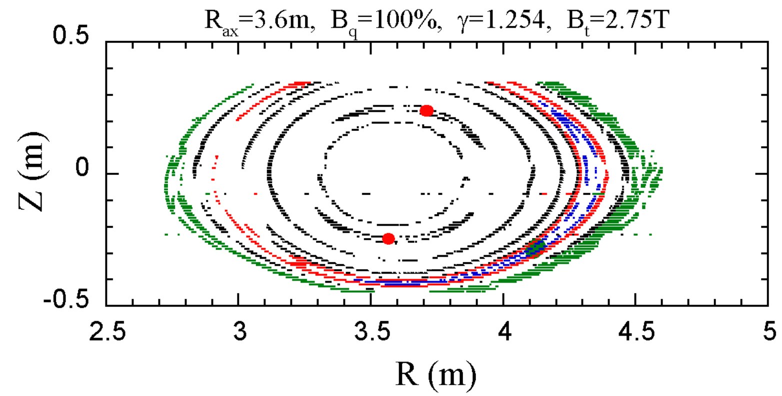

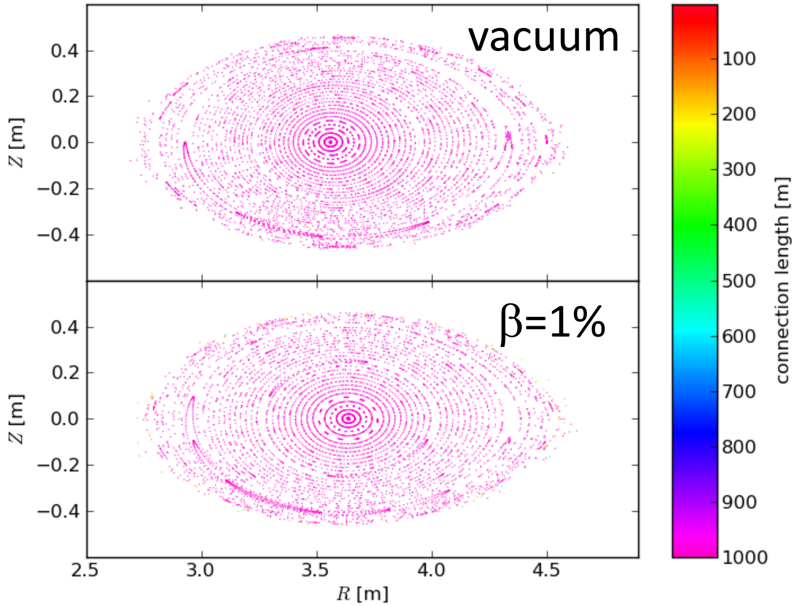

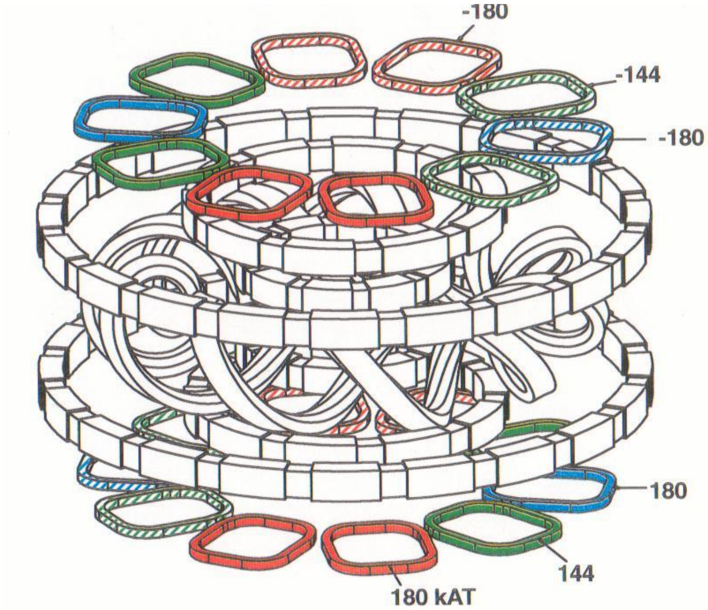

Magnetic shear is controlled by NBCD

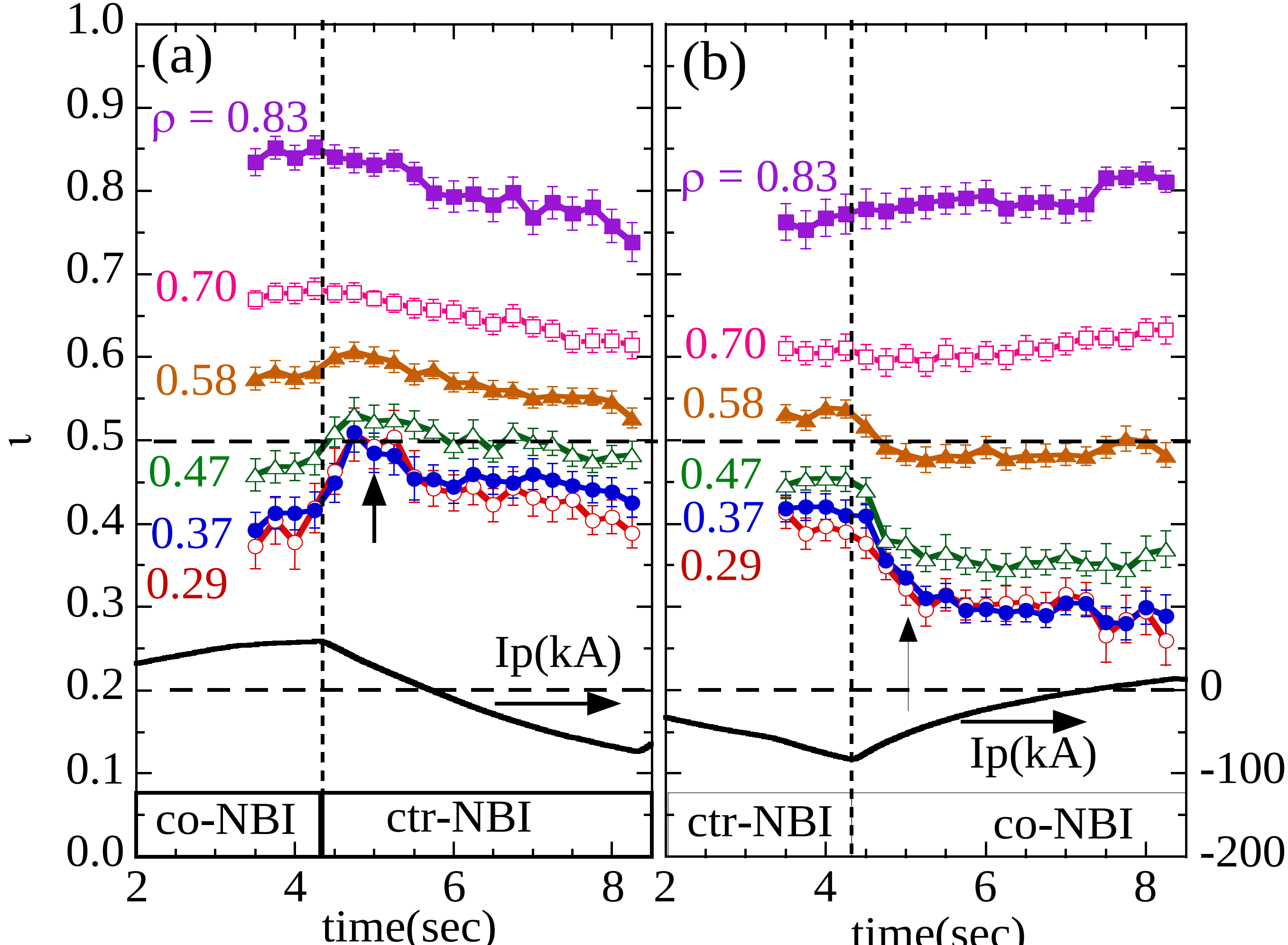

Co to ctr

Weak magnetic shear

Ctr to co

strong magnetic shear

Co= increase iota
Ctr=decrease iota

The magnetic shear can be scanned in the wide rage by switching the direction of NBI during the discharge.

Flattening of Te with weak magnetic shear at rational surface of iota =0.5

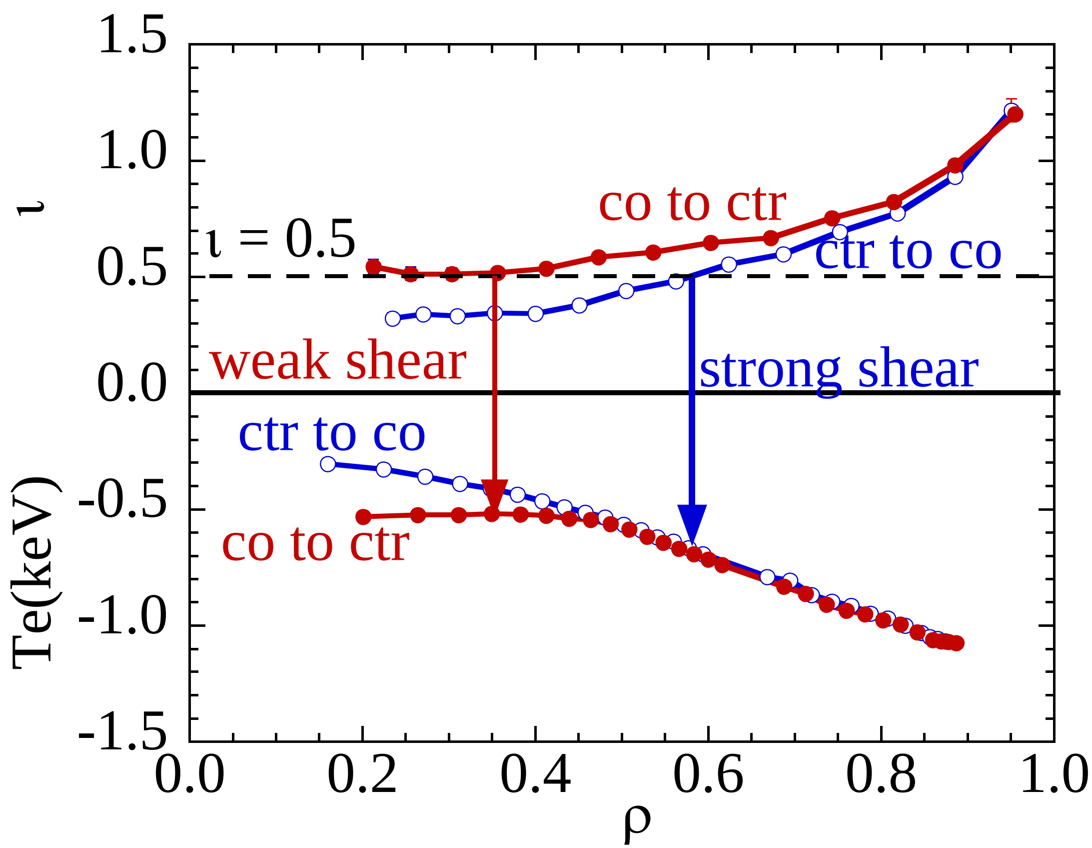

The flattening of electron temperature profile is observed in the discharge with the switch of NBI from of co- to counter, where the magnetic shear becomes weak.

Magnetic structure near the rational surface

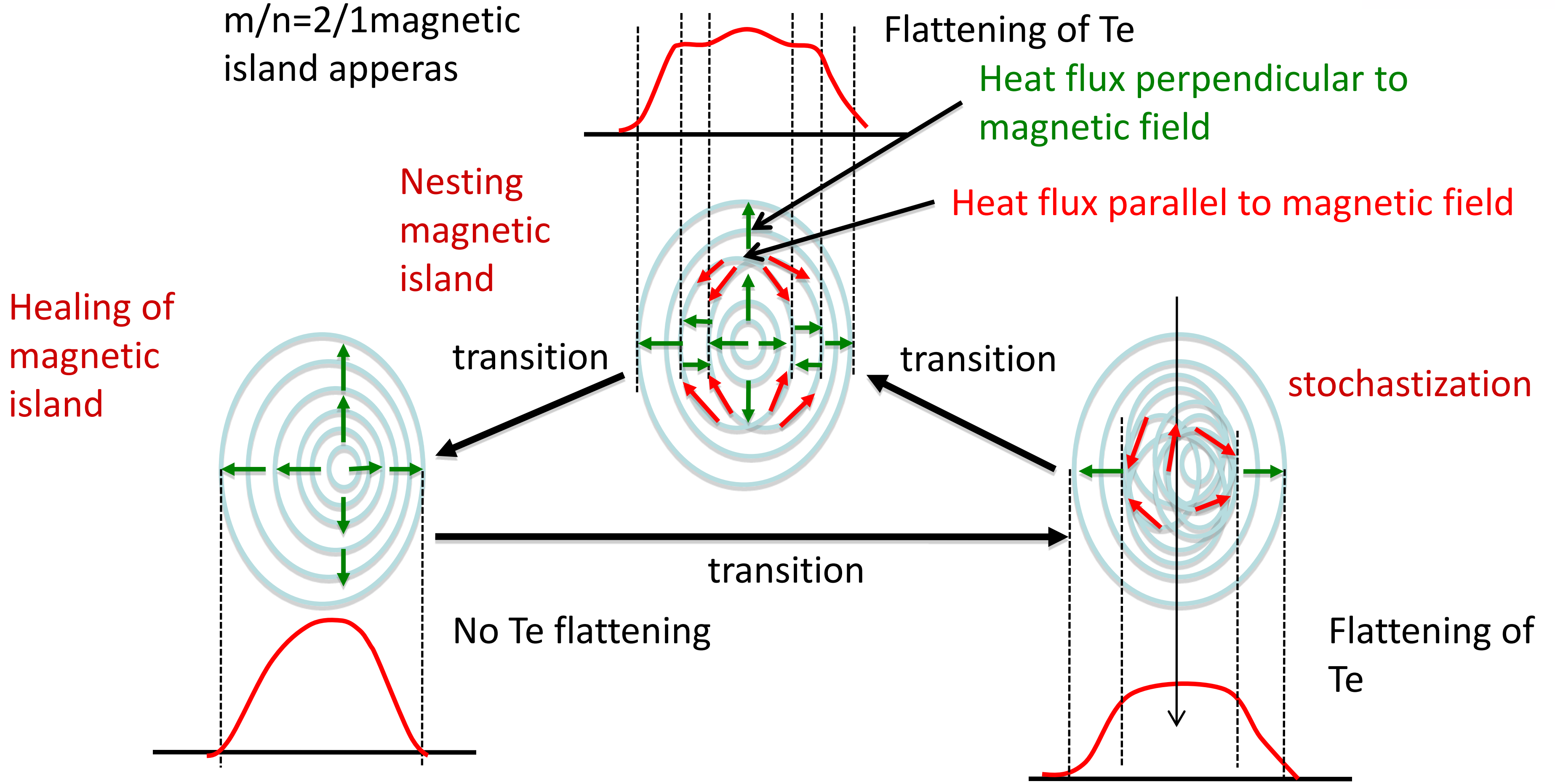

Flattening of Te ←stochastization but NOT Flattening of Te → stochastization

Heat flux parallel to magnetic field is much larger than Heat flux perpendicular to magnetic field.

The stochastization can be identified by the cold and heat pulse propagation experiment.

Fast pulse propagation is the evidence of stochastization of magnetic flux surface.

Heat pulse propagation

The direction of NBI is switched from co- to counter- during the discharge

Edge iota decreases and central iota increases, which results in weaken the magnetic shear.

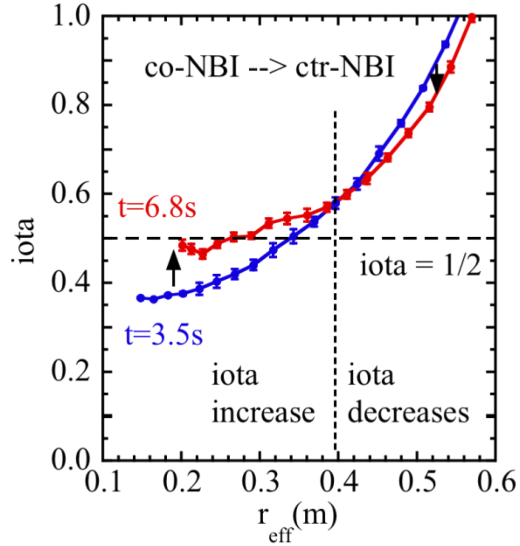

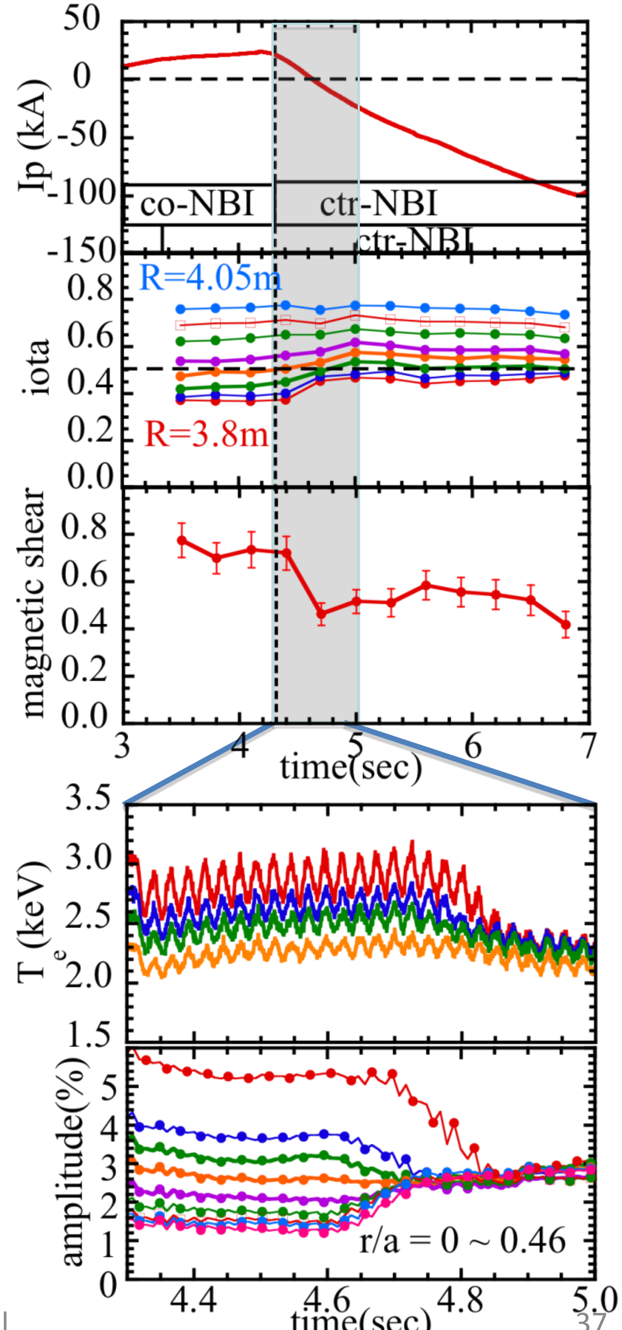

Heat pulse propagation has been studied with modulation electron cyclotron heating

Flattening of electron temperature and modulation amplitude is observed

Modulation amplitude on-axis decreases

Modulation amplitude off-axis increases

Heat pulse propagates very quickly towards the plasma edge.

Bifurcation phenomena of magnetic island

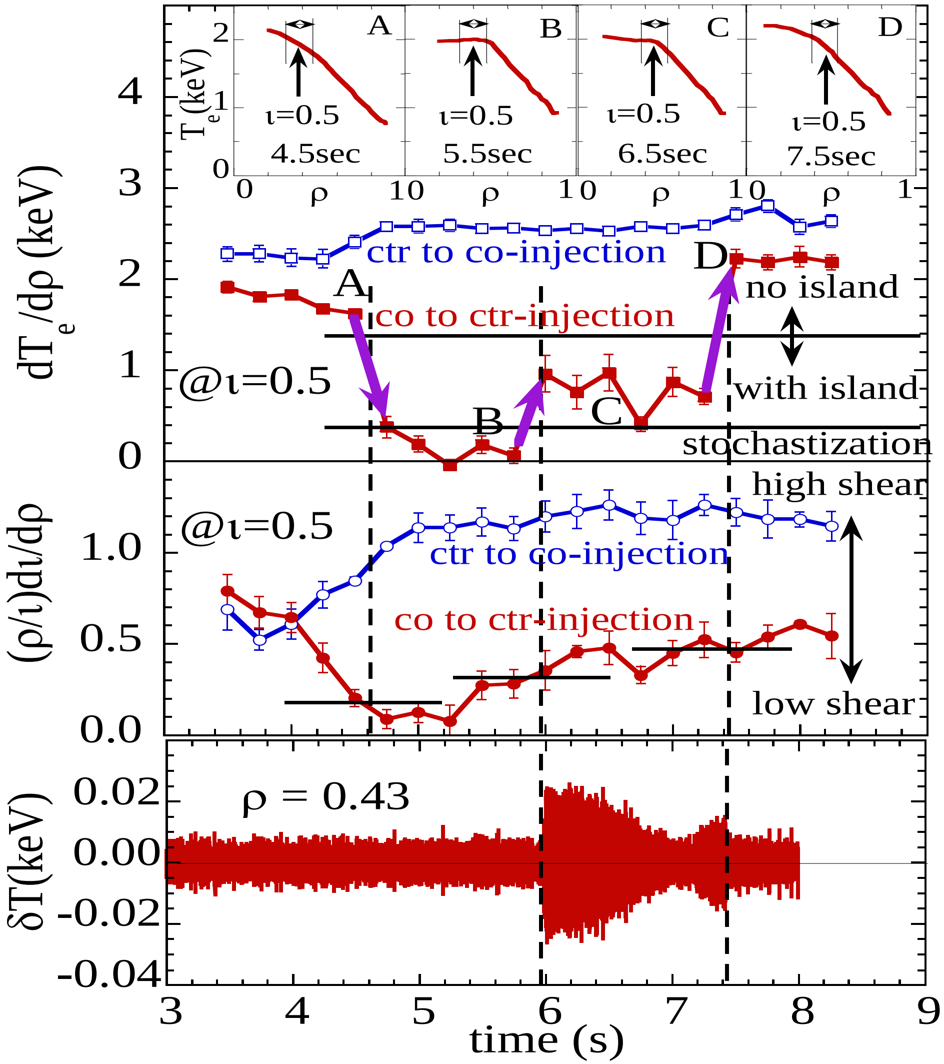

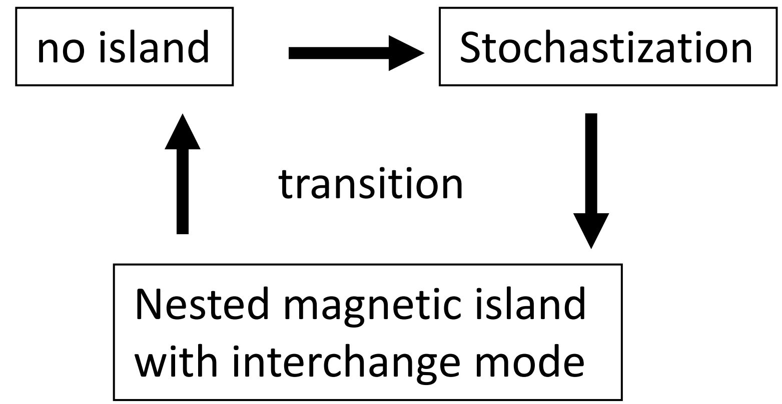

There is no MHD instability observed at the onset of temperature flattening.

The temperature fluctuations in the frequency range of 0.8 - 1.2kH appears afterwards with a partial temperature flattening

Relation of island width to magnetic shear

Island healing → island stochastization:
no interchange mode
stochastization → nesting island → healing
interchange mode is excited

Clear hysteresis is observed
In the relation between island width
and magnetic shear

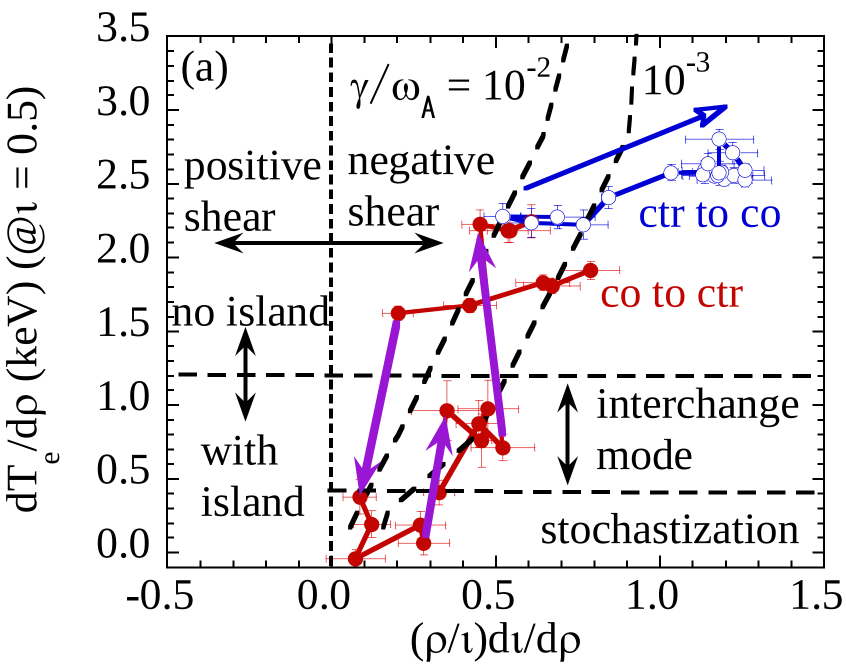

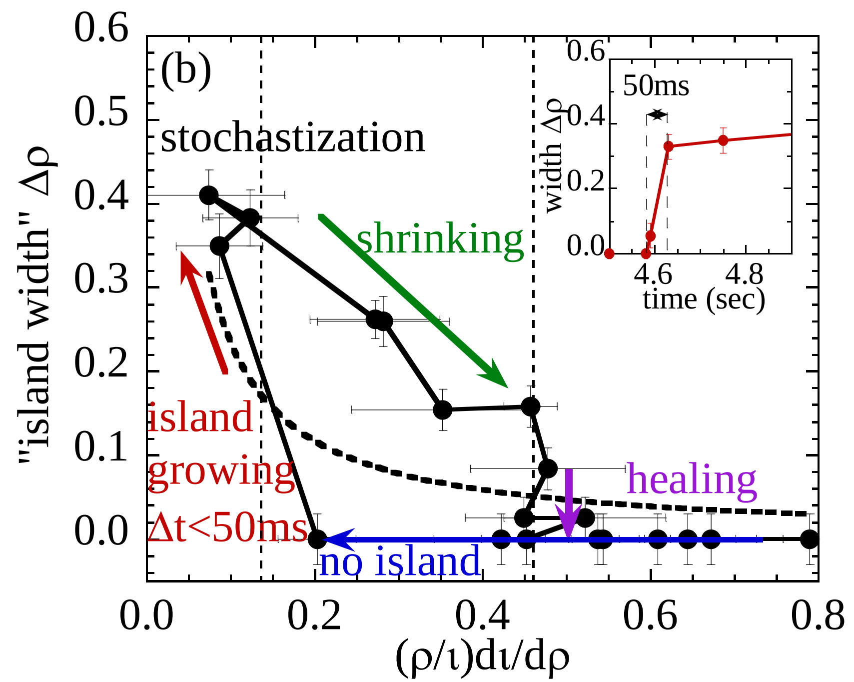

K.Ida et al., Phys. Rev. Lett, 100 (2008) 045003

Relation of island width to magnetic shear

Island healing → island stochastization:
no interchange mode
stochastization → nesting island → healing
interchange mode is excited

Clear hysteresis is observed
In the relation between island width
and magnetic shear

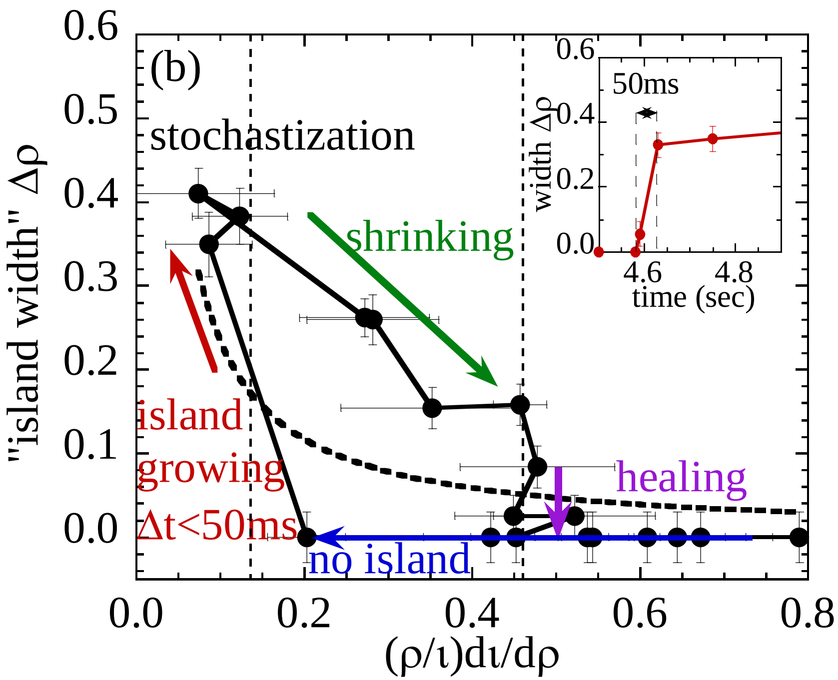

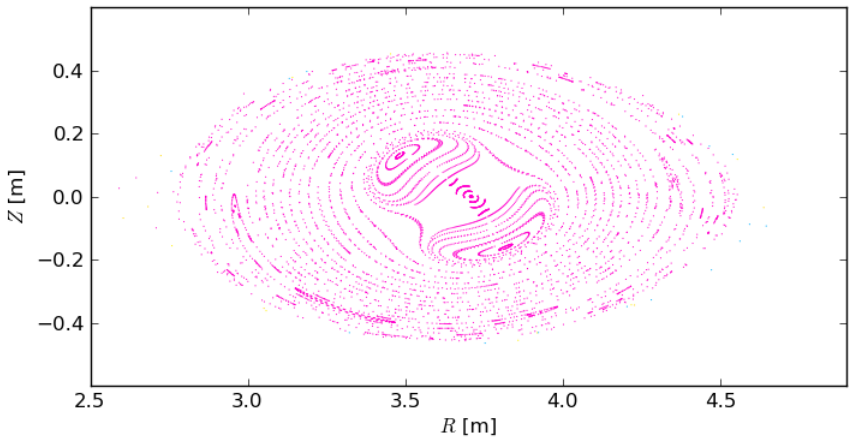

4 . 3D MHD instability studies

4.1 Magnetic shear control experiments

Configurations for Magnetic Shear Effect

γ_c (= $5a_c/R_0$) was controlled at fixed R_{ax} (3.6 m) for changing the magnetic shear on ι = 1 resonance

- Reduction of γ_c decreases the magnetic shear and V'' on the resonance
- Optimal γ_c for high-β was 1.20 because of high heating efficiency due to reduction of Shafranov shift

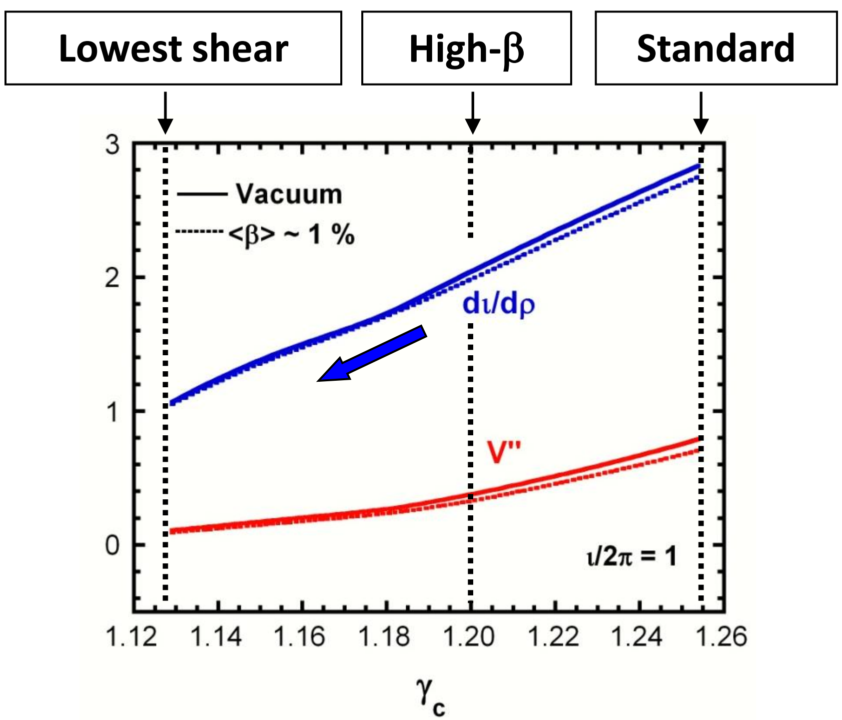

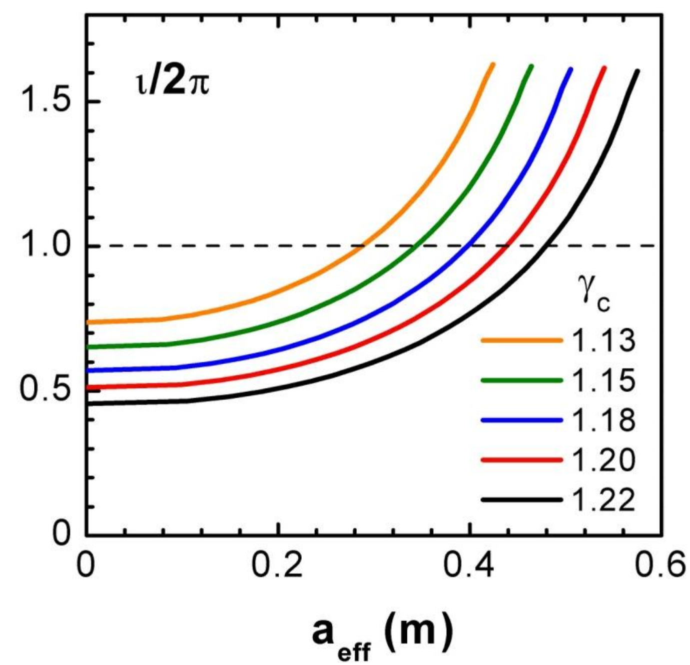

Characteristics of *m*/*n* = 1/1 mode

I_p decreasing the magnetic shear destabilizes the mode

Clear dependence of *S* on saturated mode.

$w_{1/1} \propto S^{-1/3}$ at fixed β

S.Sakakibara,

FS&T 2006, PPCF 2008

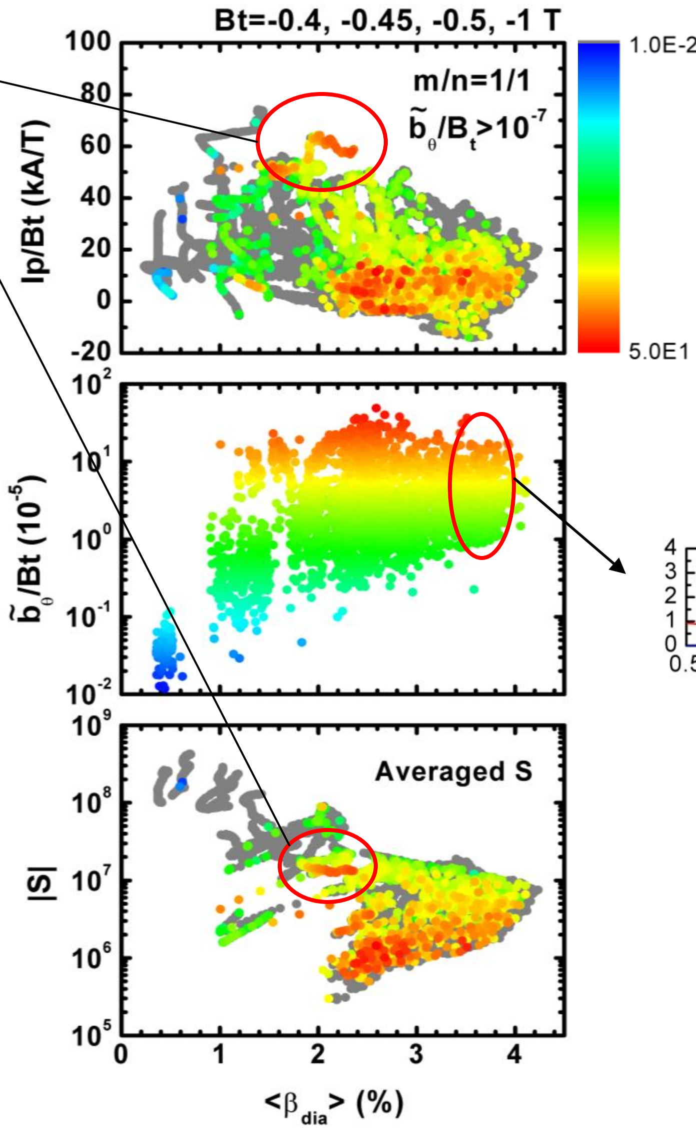

Condition:

R_{ax} = 3.6 m, γ_c = 1.20,

B_t = 0.4 ~ 1 T, H_2-puff

NBI#1, 2, 3, P_{NBI} < 12 MW

Amplitude of the mode increases with <β> and p-gradient in the <β> < 3 % range.

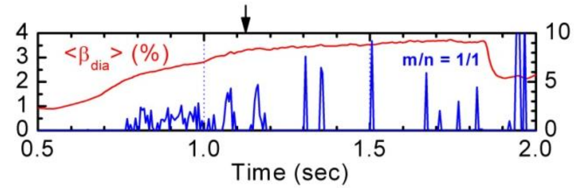

Fluctuations change from continuation to intermittent with the profile flattening, in the high-β regime

A.Komori & S.Sakakibara,

PoP 12 (2005)

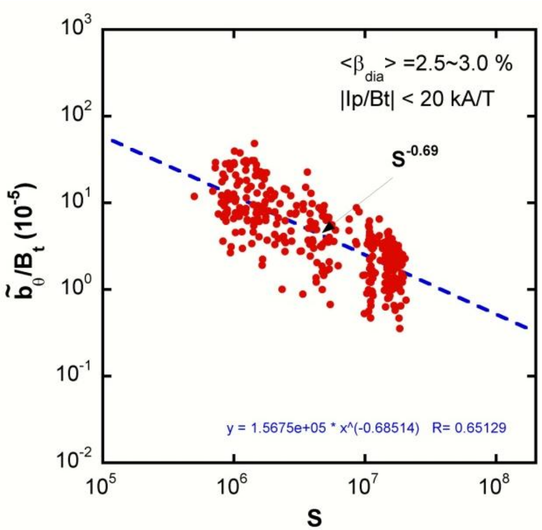

Occurrence of Non-Rotating Mode

- Large m/n = 1/1 mode without rotation appeared in γ_c = 1.13 configuration
- ideal unstable regime ($D_I > 0$)

S.Sakakibara, FS&T 2006

- The mode caused T_e profile-flattening around the resonance
- Plasma current decreasing magnetic shear enhances the mode activity further.

$\Rightarrow$ magnetic shear effect

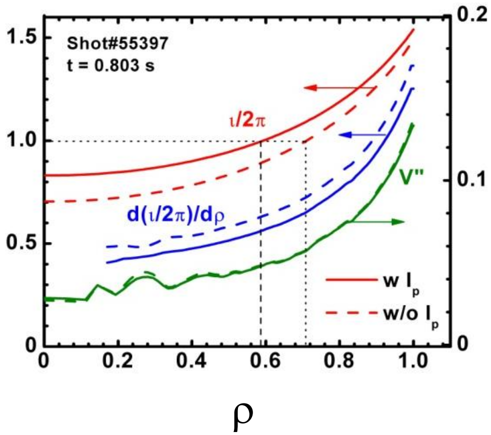

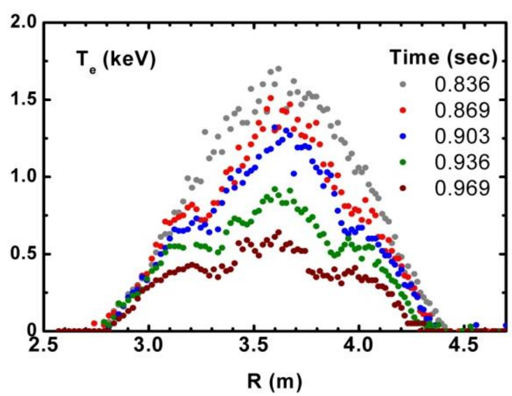

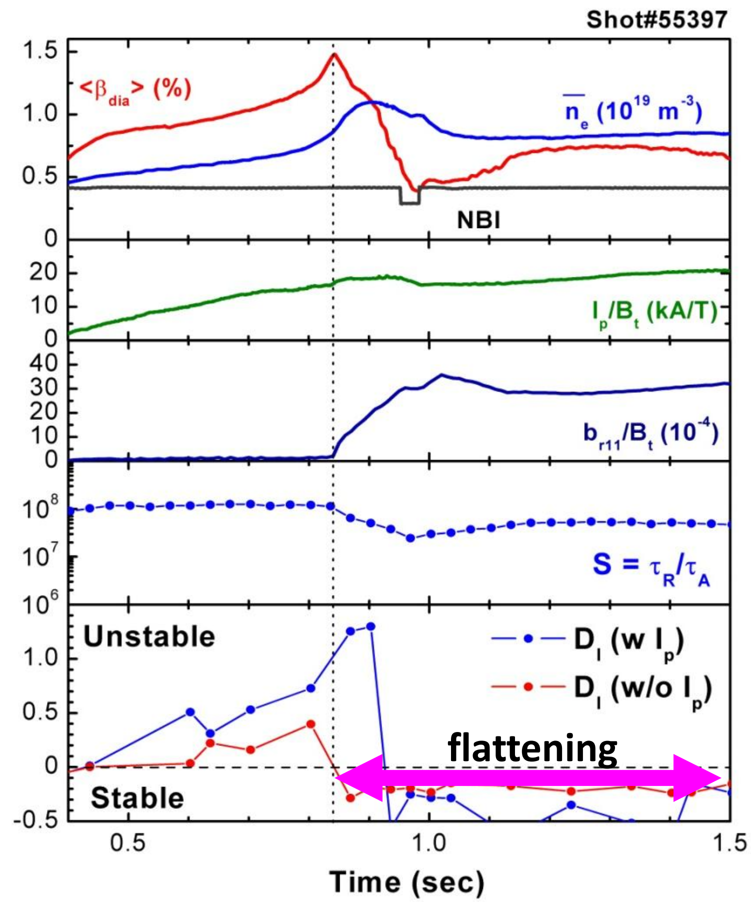

Radial Magnetic Flux Measurements

- 24 saddle loops (2 arrays) have been installed inside vacuum vessel for measuring magnetic flux due to equilibrium currents and locked mode.
- Two arrays are at intervals of 180 deg.
- Dipole field profile has n = 10 periodicity

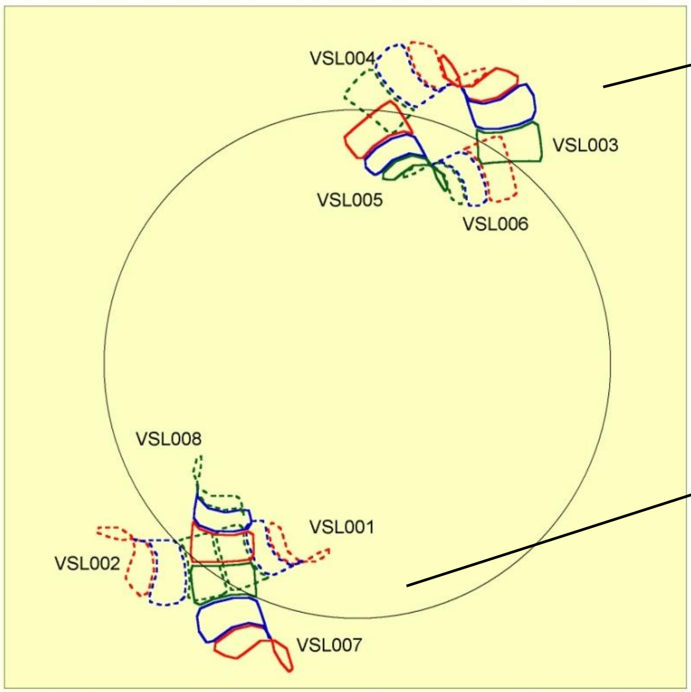

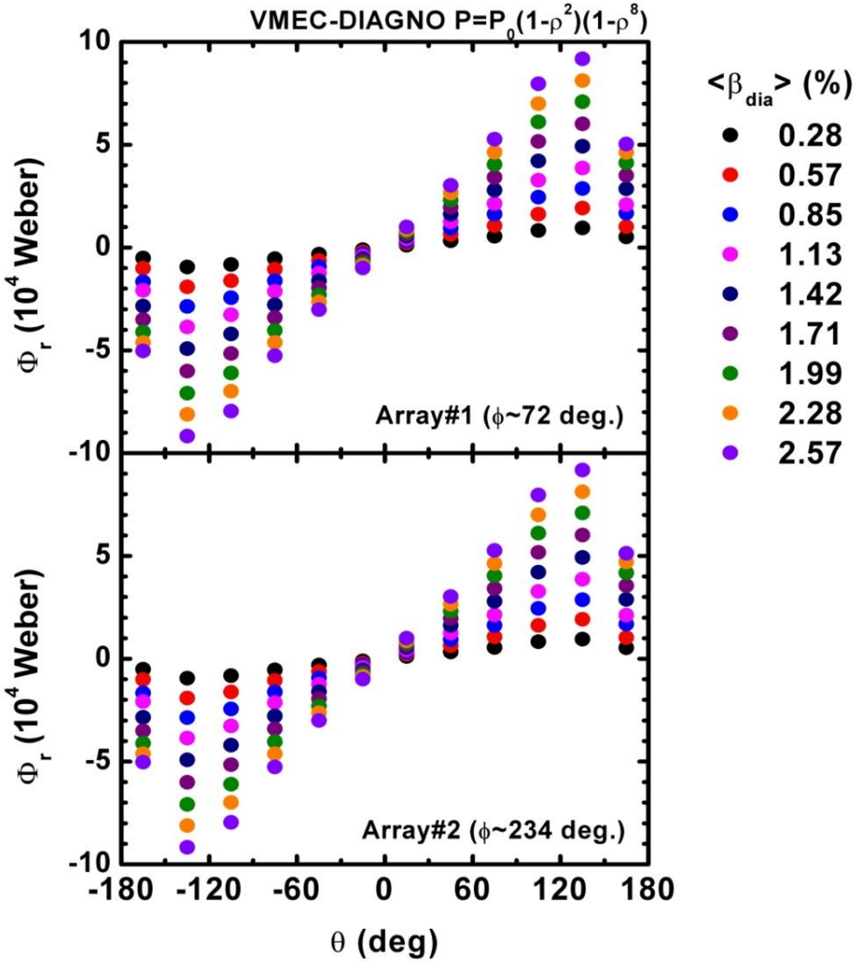

Appearance of the Mode

- Minor collapse occurs at 0.82 s
- Then toroidal periodicity of flux profile is suddenly broken.

Before

Growth

Saturation

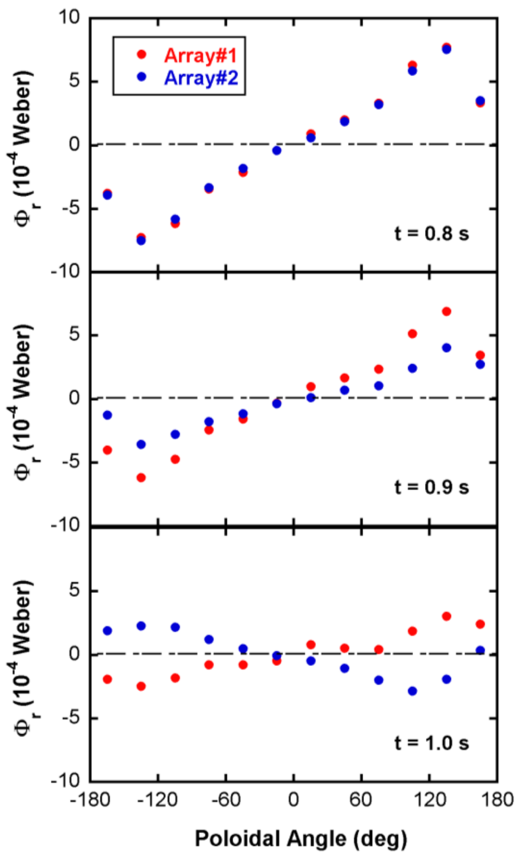

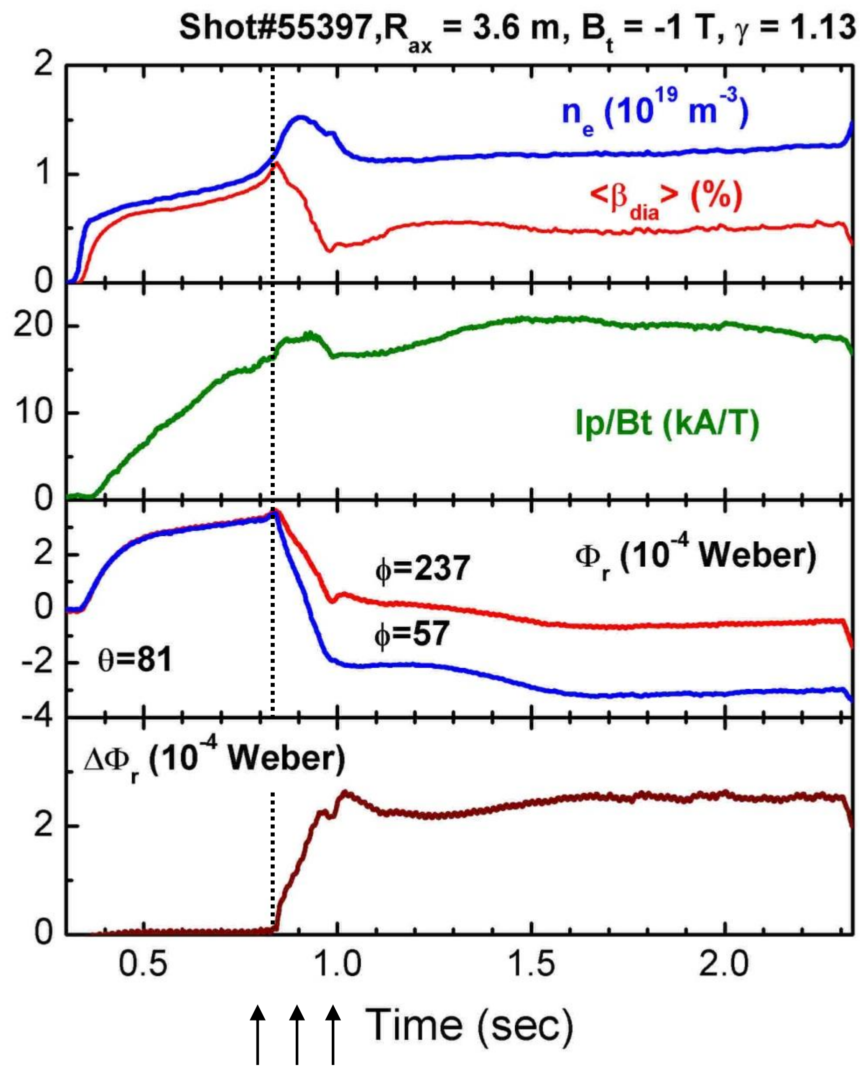

Technique of Flux Analysis

- Comparison between measured DF$_r$ = $F_{r1} - F_{r2}$ and DF$_{1/1}$ calculated by multi-filament method

- b_r component on the resonance $\boldsymbol{b_r = m_0/4p^*I_s/r_s}$ and spatial position of the mode can be estimated

Boozer Coordinates (VMEC)

$R(\mathrm{r}) = \Sigma R_{mn}\cos(mq_B - nf_B)$

$Z(\mathrm{r}) = \Sigma Z_{mn}\sin(mq_B - nf_B)$

$f(\mathrm{r}) = \mathrm{f}_B\Sigma f_{mn}\cos(mq_B - nf_B)$ $i/2p$

$= f_B / \vartheta_B$, $m = km'$, $n = kn'$ (k: degree)

$N_{fil}m'$ (f direction)、N_{fil}/m' (q direction)

fil.current : $\mathrm{I} = \mathrm{I}_s\cos(mq_B - n f_B + \boldsymbol{a})$

$I_s = N_{fil}mI_{fil}$

Estimated b_r is likely to be produced by …

- difference of PS profiles

- instability

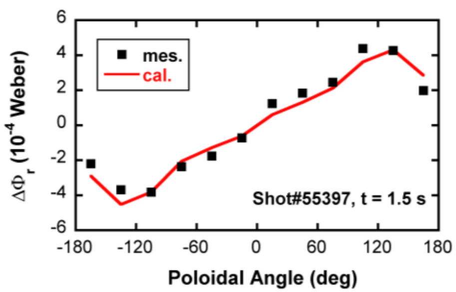

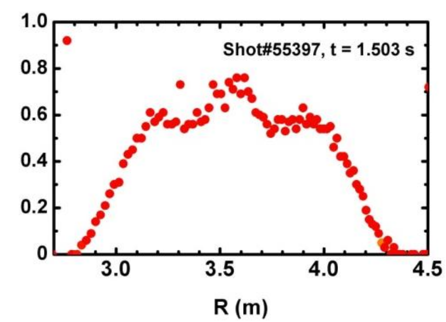

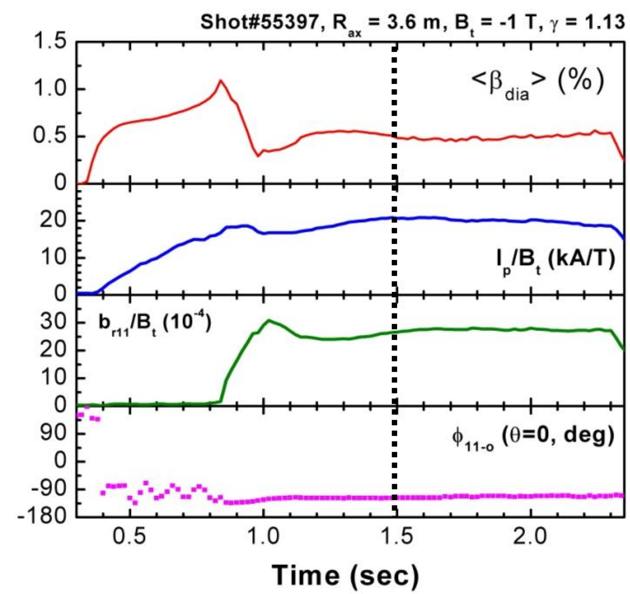

γ_c and I_p Dependences of the mode

- Appearance of the mode obviously depends on γ_c and I_p
- The mode appears even in high- γ_c if I_p exceeds a threshold.
- A threshold of the plasma current decreases with decreasing γ_c
- Operation limit is qualitatively consistent with ideal theory

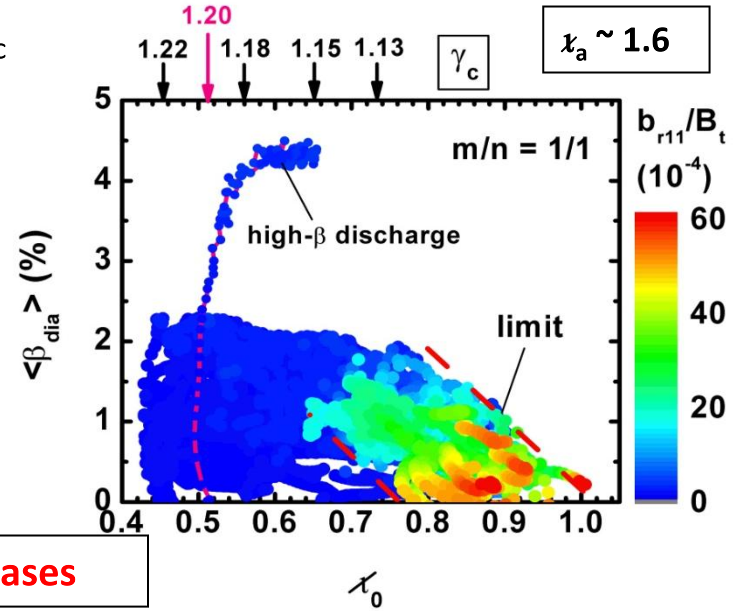

Magnetic shear decreases

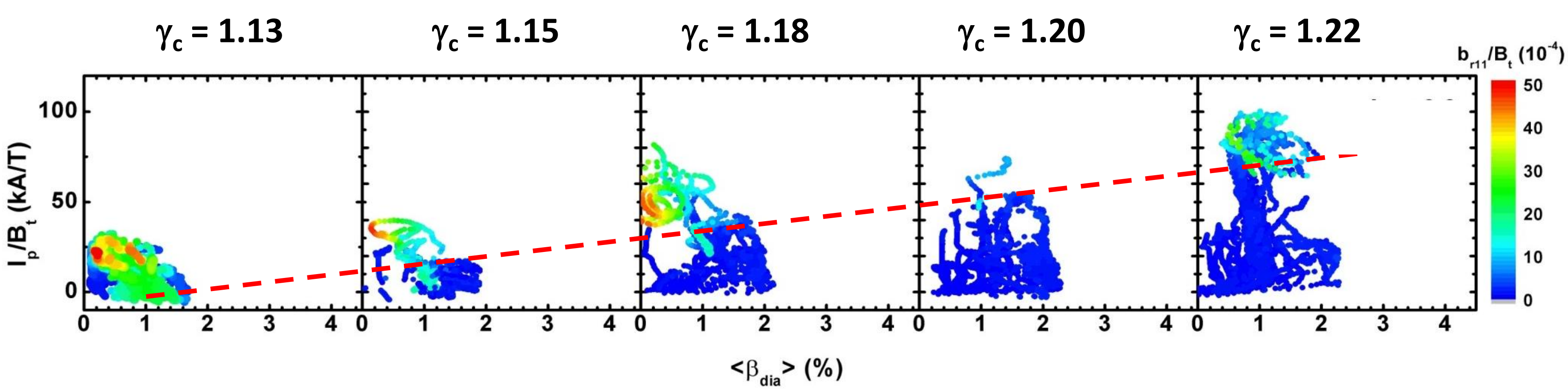

Plasma rebounded against "Limit"

- Even if γ_c is sufficiently high, the I_p causes the minor collapse
- Plasma is rebounded from "limit" three times.

$\gamma_c = 1.22$

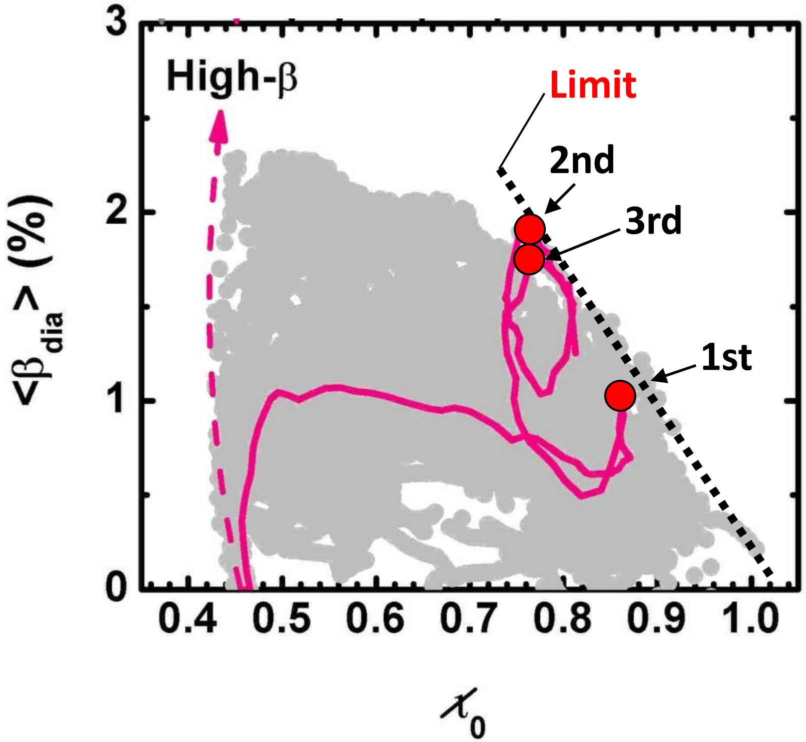

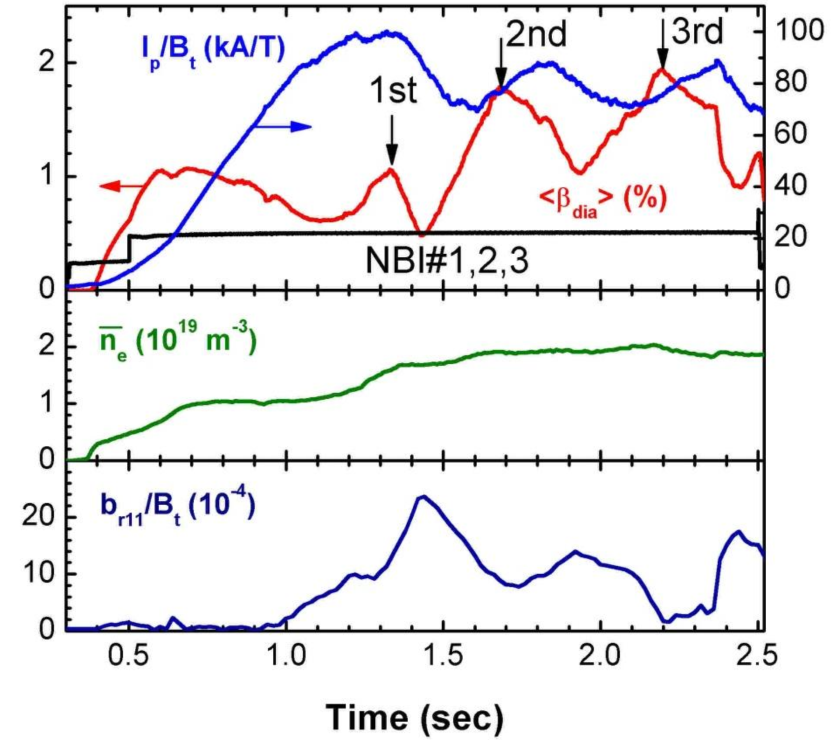

Counter Ip experiment

• Magnetic shear is essential for excitation of the mode?

  ⇒ counter-I_p experiments (Nov.2,2005)

• Sawtooth-like Oscillation was observed, and the inversion radius identified by FIR signals is located around ι/2p = 1

• Φ_r signals also indicate that the *n* number is odd

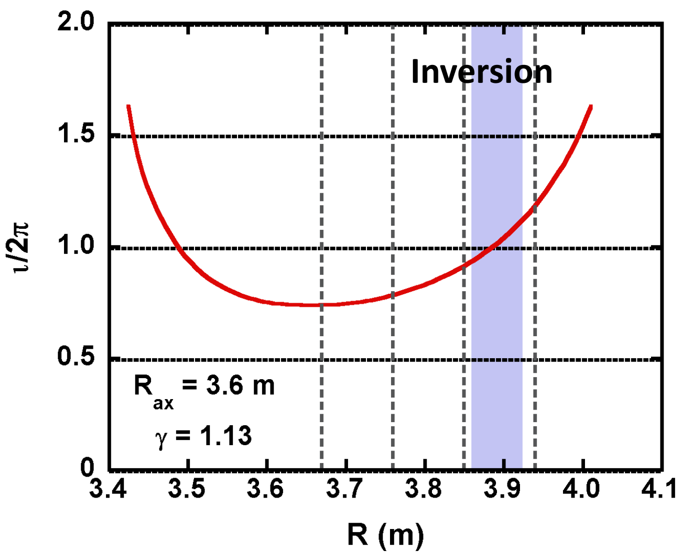

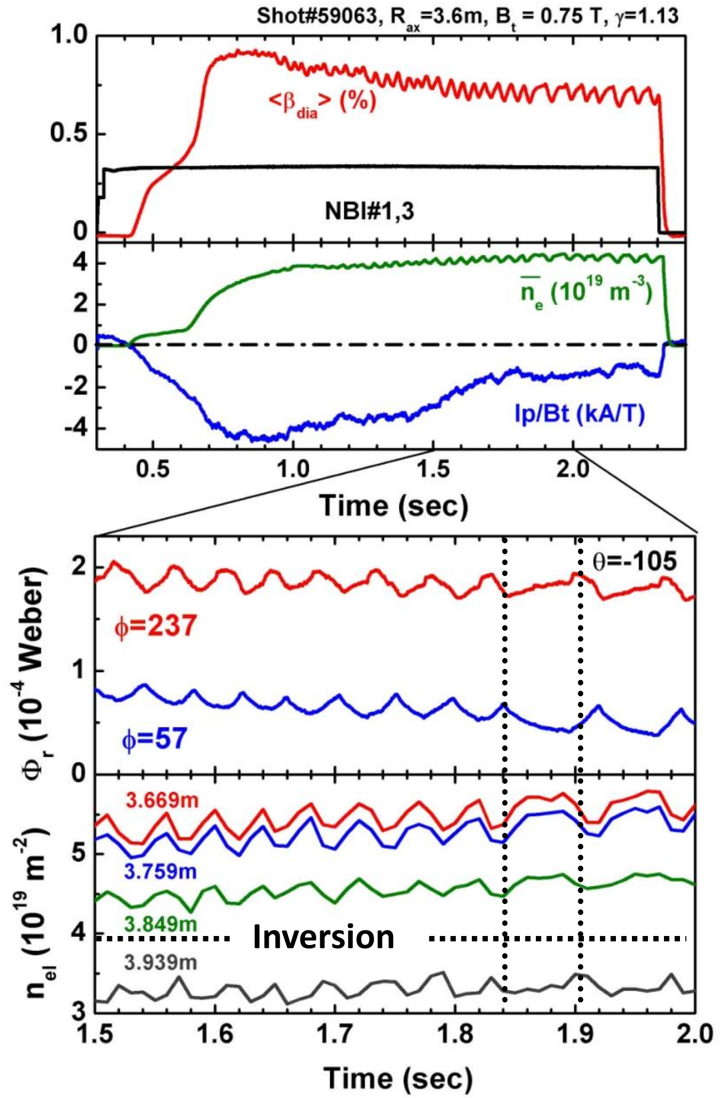

Verification of I_p effect on 1/1 mode

- ST amplitude increases with the decrease in the counter current.
- Plasma exists near "onset" region of the *m*/*n*=1/1 mode.
- Toroidal location of the mode does not depend on the direction of B_t.

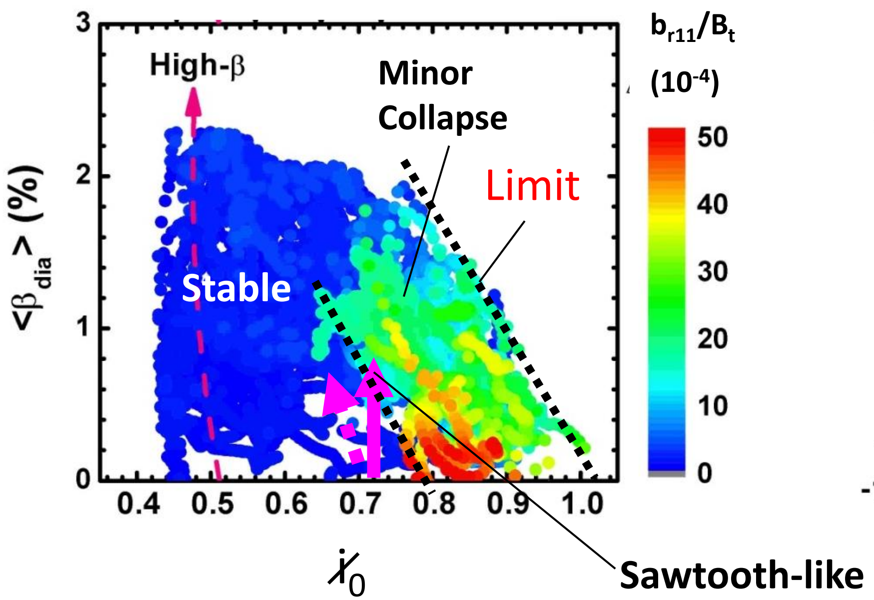

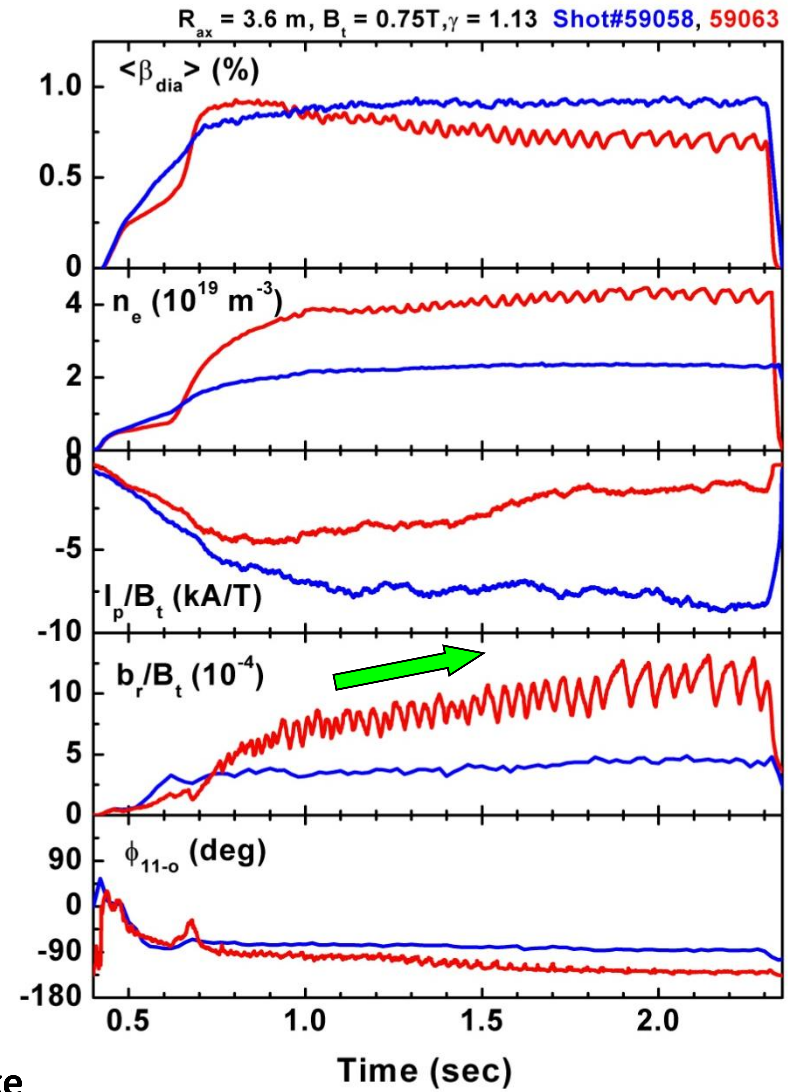

Specification of PC Power Supply

Capacity of PC PS was increased

- IS, IV coils : < 6. 2 kA
- H 45 V, P 213 V (SS H 45 V, P 33 V)
- Operation with ≤ 1.5 T is available
- Fixed B_t or Fixed I_{HC} operations

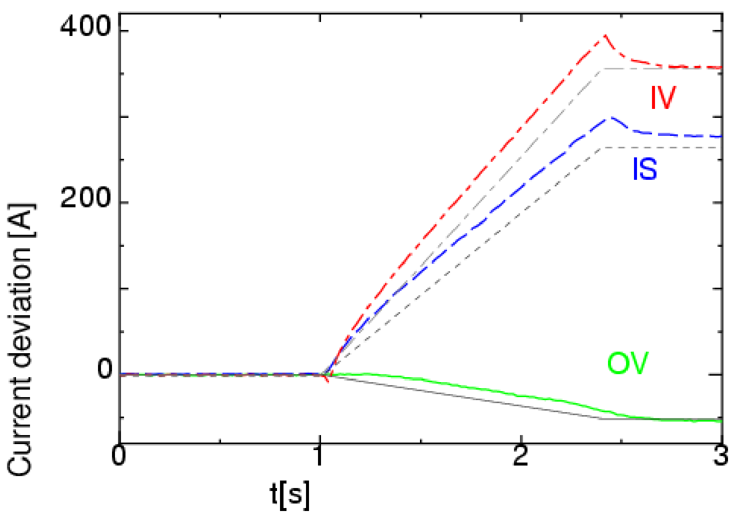

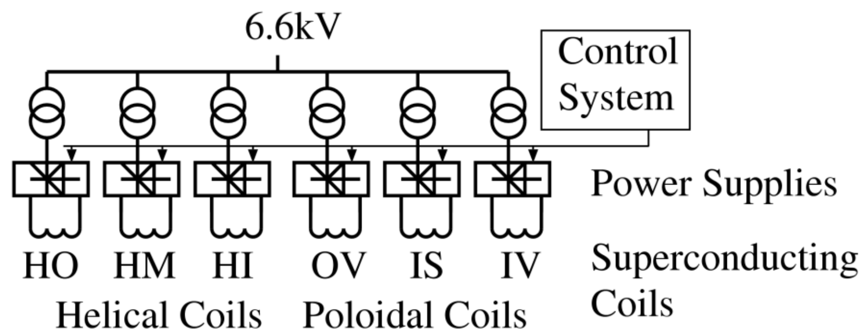

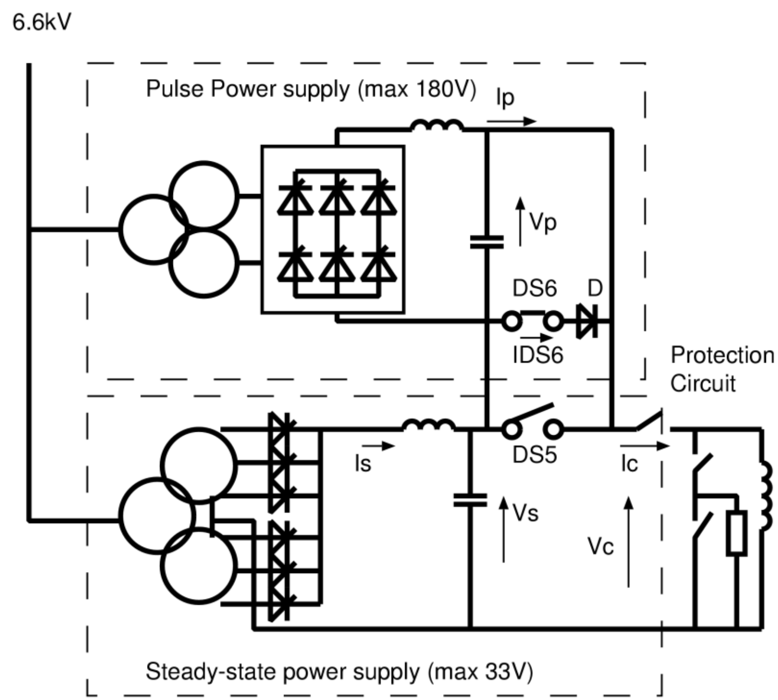

Example of R_{ax} Swing Discharge (2.0 sec)

Reference

R_{ax} = 3.6 m, B_t = -0.425 T, γ_c = 1.20

NBI#1,3 (Co.,1.3 s~) NBI#2 (Ctr., 1.8s~)

R_{ax} Swing

R_{ax} = 3.6 m $\rightarrow$ 3.5 m for 2 sec

Both R_{ax} and R_{00} shifts with the preset

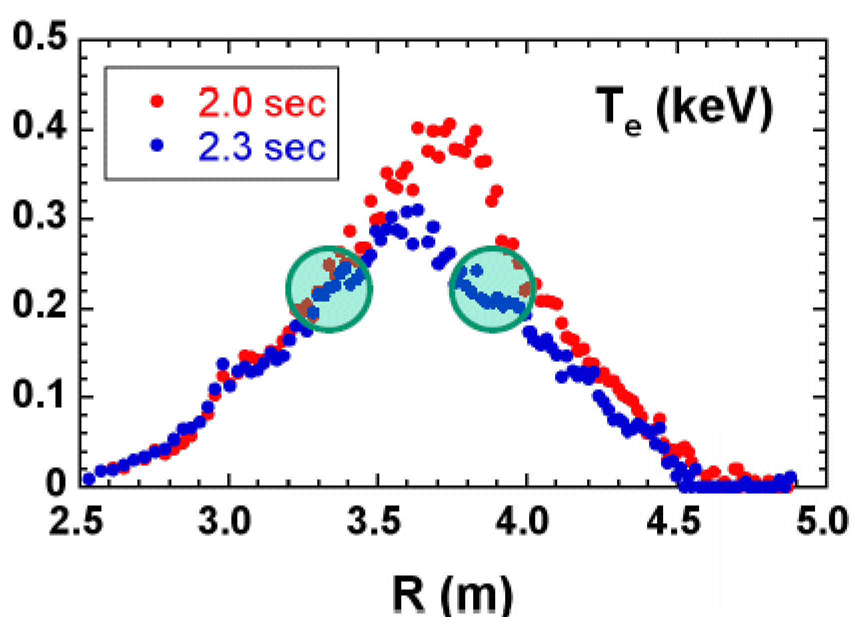

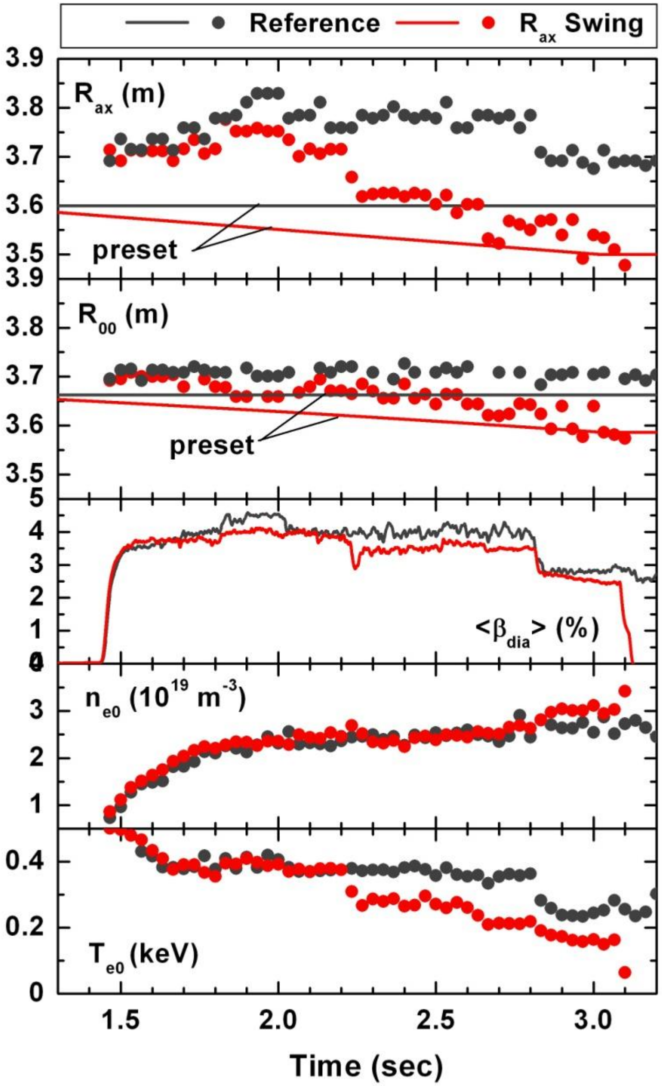

Characteristics of m/n = 1/1 mode

Several differences of characteristics of the mode between "*non-rotating*" and "*rotating*" modes:

	"*non-rotating*" mode (low-γ_c, large I_p)	**"*rotating*" mode** (Standard, high-β)
radial location	$\rho \sim 0.7$ (currentless)	$\rho \sim 0.9$
configuration	weak shear, magnetic hill	magnetic hill
observation	$D_I > 0$, $D_R > 0$	$D_I < 0$, $D_R > 0$
frequency	DC ~ several Hz	several kHz
spatial location	$\phi \sim -120$ deg (near natural error field)	rotating
S dependence	Not clear	strong

Interaction of the modes with Resonant magnetic field

4 . 3D MHD instability studies

4.2 Interaction with magnetic islands

Interaction with "*Rotating*" Mode

• Finite pressure gradient /near $\iota = 1$ surface exists till $I_{LID} \leq 220$ A/T, whereas it gradually decreases with I_{LID}.

• Amplitude of the mode decreases with reduction of the gradient, and the mode disappears despite finite gradient still remains.

Then the mode frequency slowed down

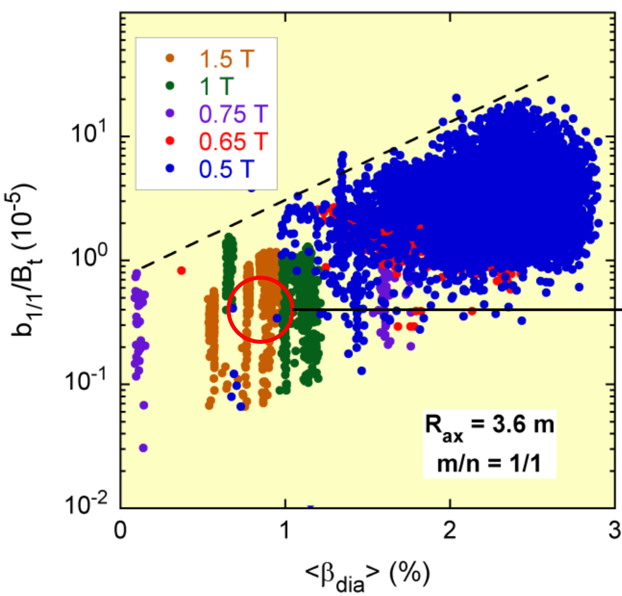

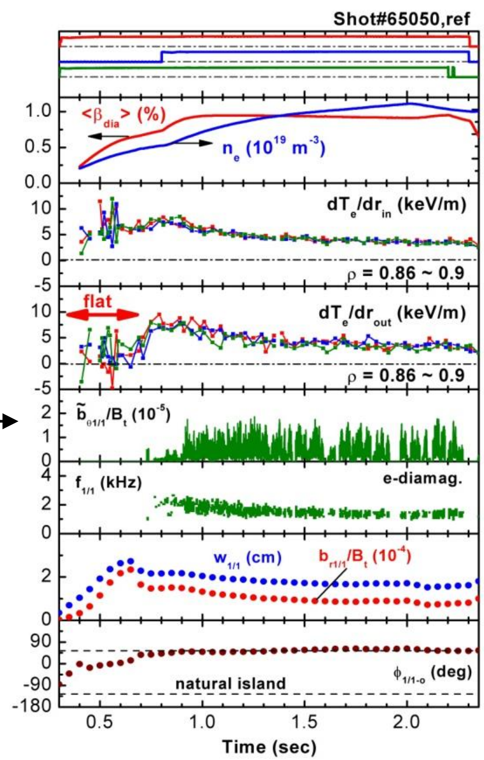

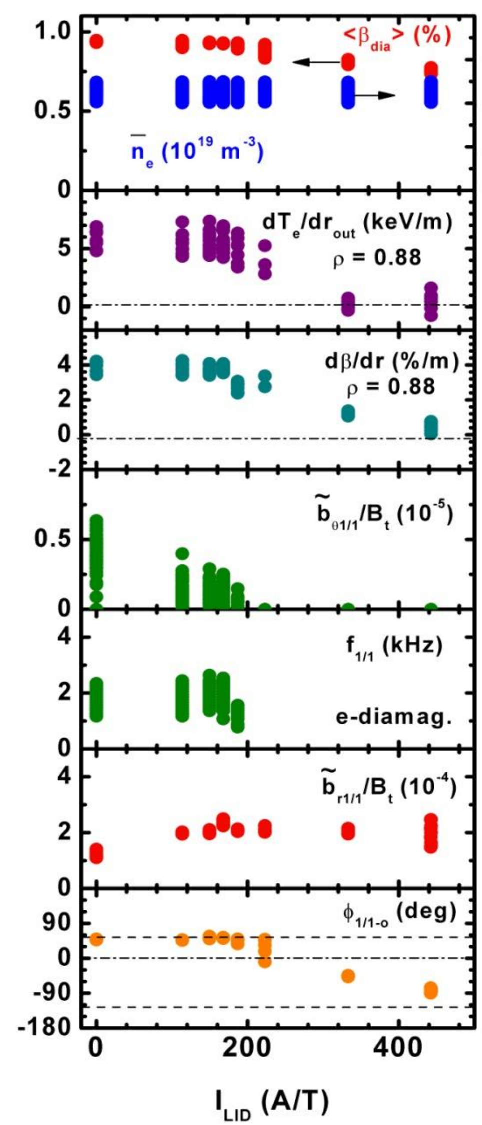

Interaction with “*Non-Rotating*” Mode

- The mode could be completely suppressed by giving optimal island width, and <β> recovered.

- The location and saturation-level of the mode strongly depended on that of given static island.

- Non-linear instability like locked mode?

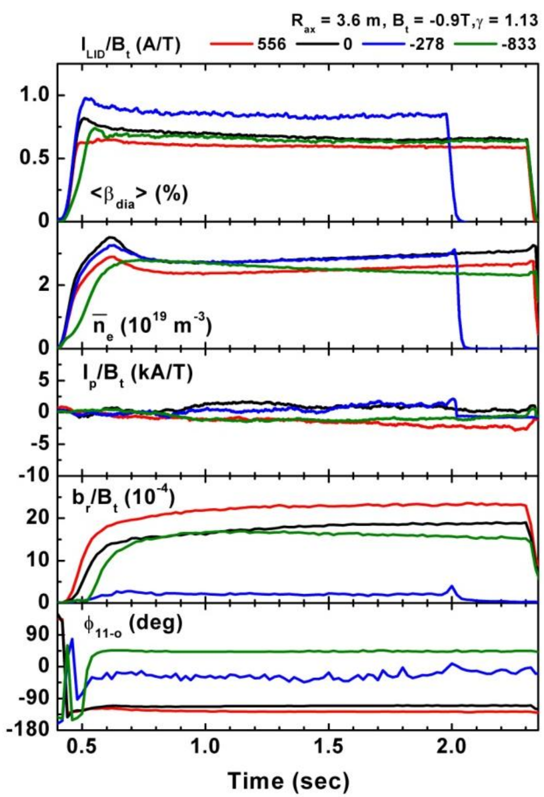

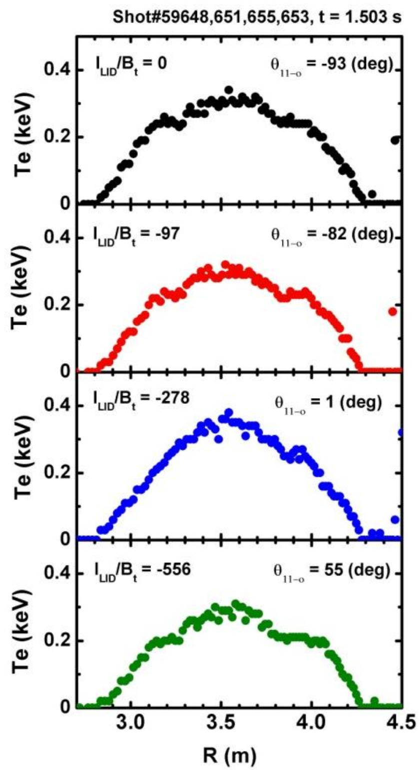

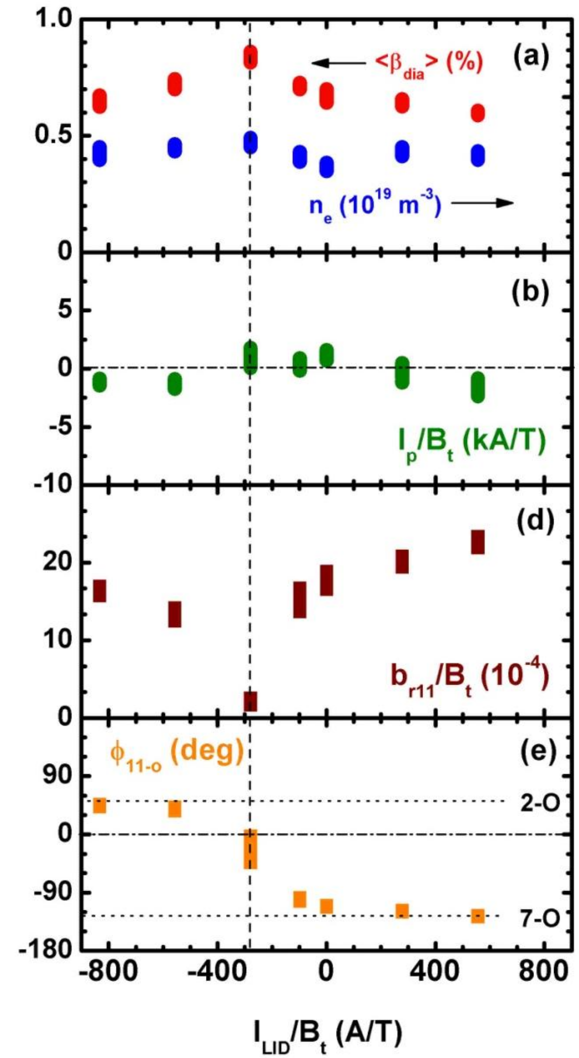

4 . 3D MHD instability studies

4.3 Core Density Collapse

Core Density Collapse

- Observed in SDC plasma
- Decreased Density
- Unchanged temperature
- Observed fluctuation in the peripheral region

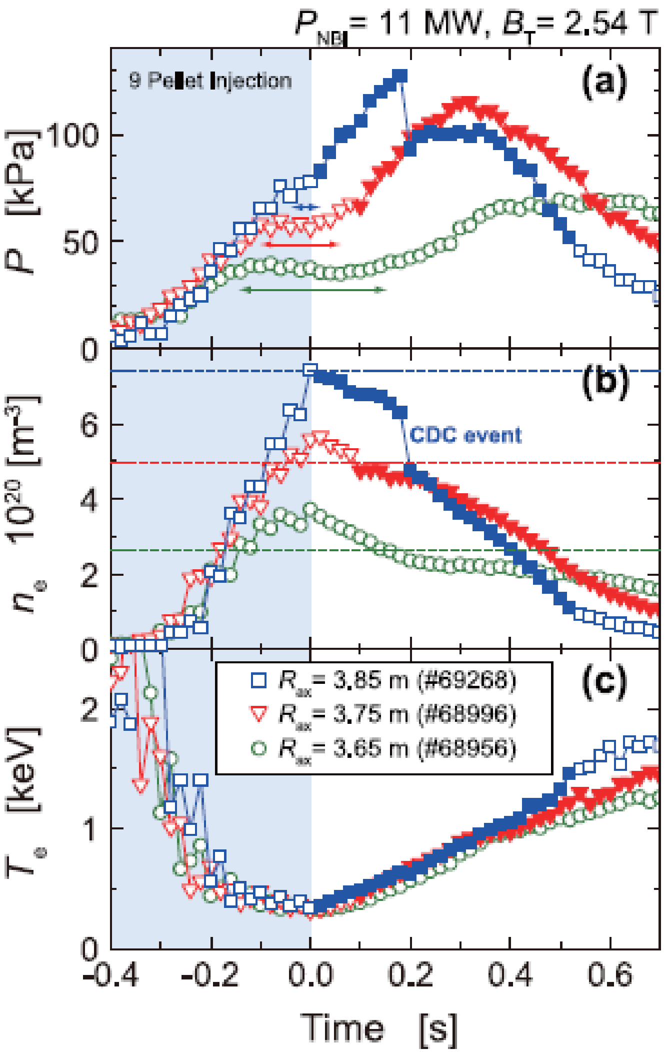

Finite-β equilibrium in a SDC Plasma

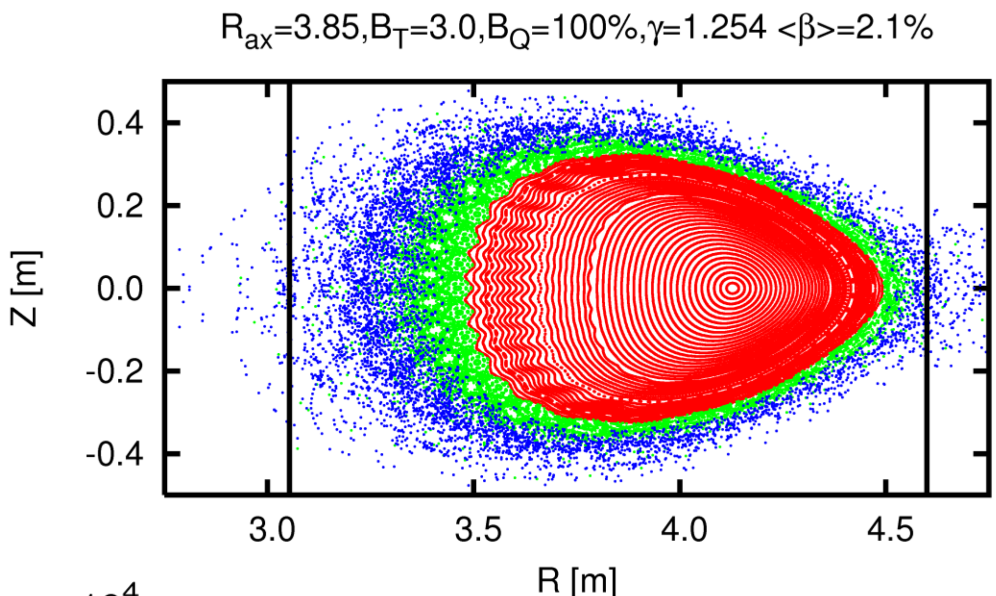

- Edge field lines are strongly ergodized.
- Field lines indicated by green do not reach to wall.
- L_C of field lines with blue is short.
- ∇T_e exists in the stochastic region.
- L_C is longer than λ_e.

These indicate the pressure can exist on stochastic field.

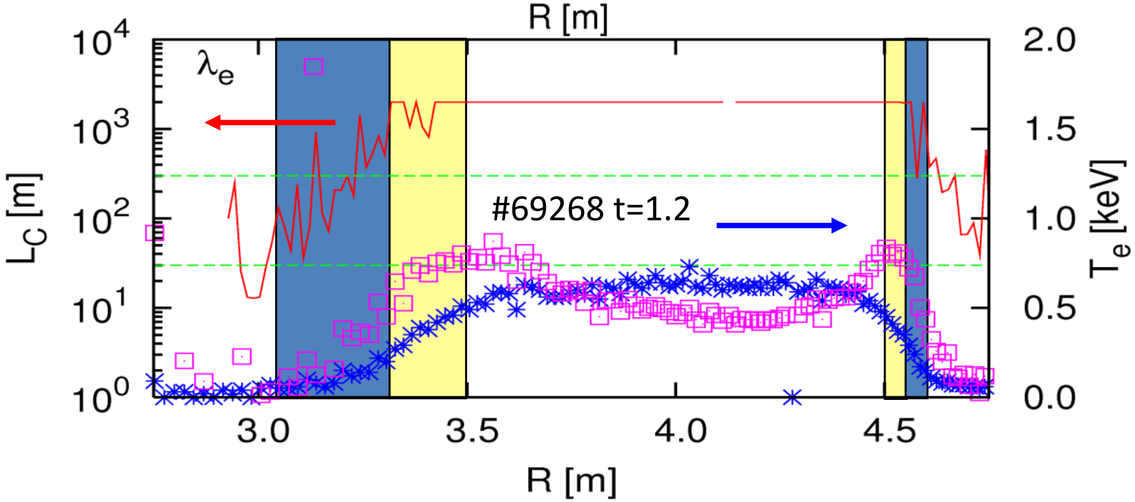

Comparison of pressure profile

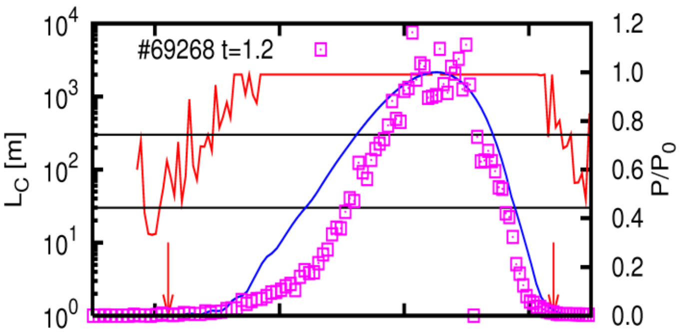

Numerical model

$$\frac{\partial \rho}{\partial t} = -\nabla \cdot (\rho \mathbf{v}) \qquad (1)$$

$$\rho \frac{\partial}{\partial t} \mathbf{v} = -\rho \omega \times \mathbf{v} - \rho \nabla \left(\frac{v^2}{2}\right) - \nabla p + \mathbf{j} \times \mathbf{B}$$

$$+\frac{4}{3} \nabla [\nu \rho (\nabla \cdot \mathbf{v})] - \nabla \times [\nu \rho \omega] \qquad (2)$$

$$\frac{\partial \mathbf{B}}{\partial t} = -\nabla \times \mathbf{E} \qquad (3)$$

$$\frac{\partial p}{\partial t} = -\nabla \cdot (p \mathbf{v}) - (\gamma - 1) p \nabla \cdot \mathbf{v}$$

$$+(\gamma - 1)[\nu \rho \omega^2 + \frac{4}{3} \nu \rho (\nabla \cdot \mathbf{v})^2 + \eta \mathbf{j} \cdot (\mathbf{j} - \mathbf{j}_{\mathrm{eq}})] \qquad (4)$$

$$\mathbf{E} = -\mathbf{v} \times \mathbf{B} + \eta (\mathbf{j} - \mathbf{j}_{\mathrm{eq}}) \qquad (5)$$

$$\mathbf{j} = \frac{1}{\mu_0} \nabla \times \mathbf{B} \qquad (6)$$

$$\omega = \nabla \times \mathbf{v} \qquad (7)$$

•4th order finite difference
•4th order Runge-Kutta method for time integration
•Grid points on the cylindrical coordinates (R,ϕ,Z)

Simulation results

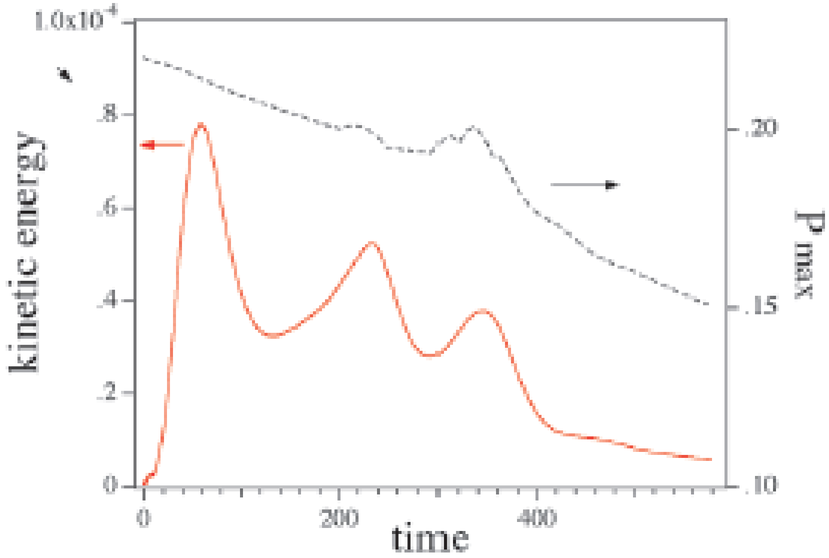

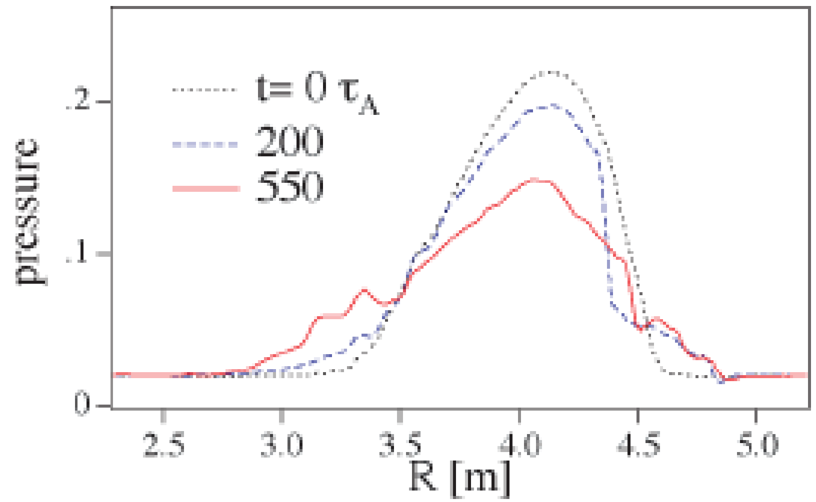

- Saturated for $400\tau_{A.}$
- After $300\tau_A$, P_{max} decreases quickly.

- Central pressure decreases.
- Edge pressure increases

Simulation results

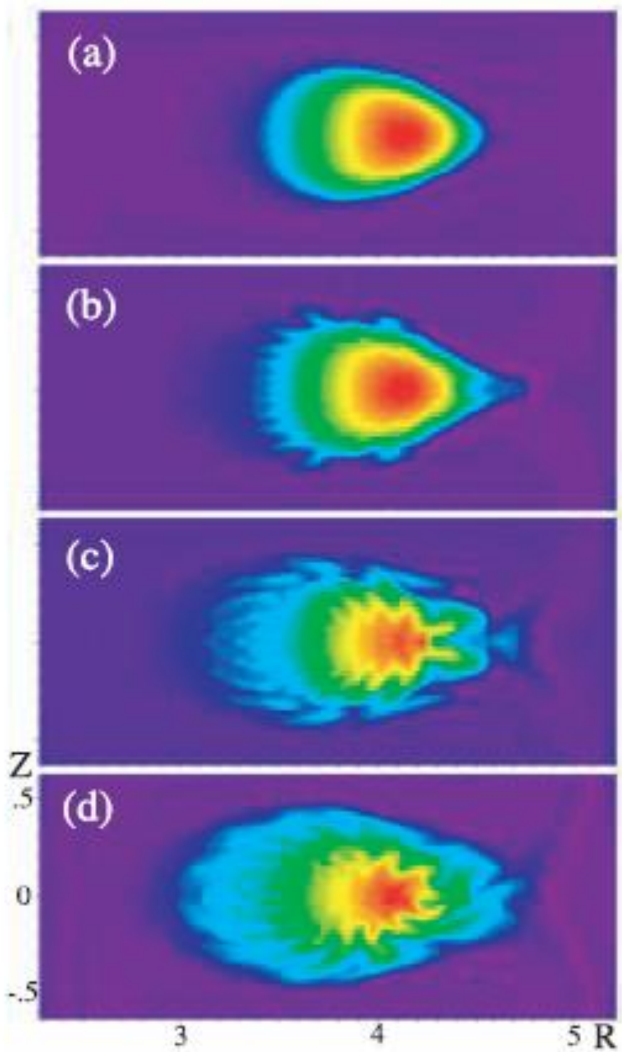

Perturbation in linear phase

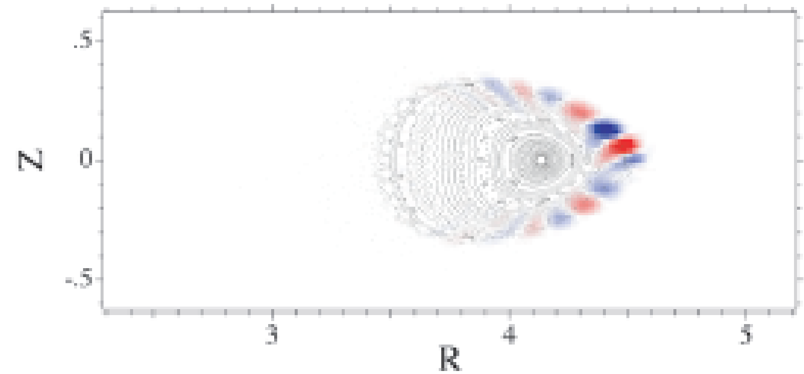

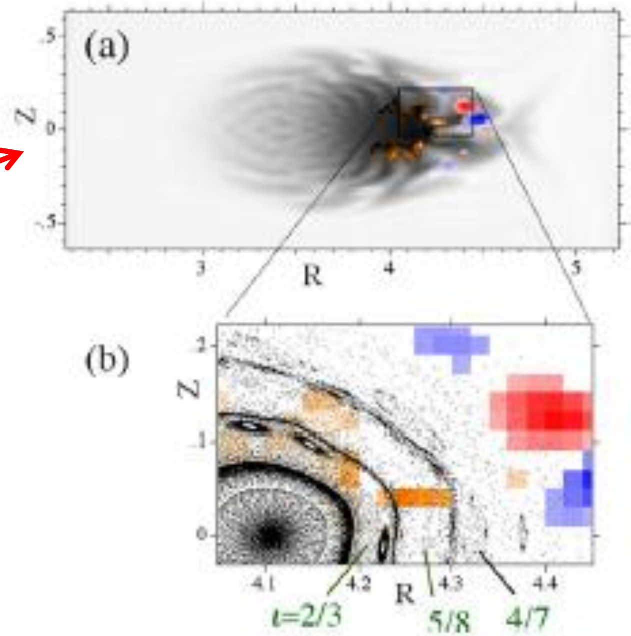

5. Application of 3D tools to Tokamaks

Applications to ITER

Plasma response to TBM ripple and coupling Ferrite insert are urgent issues.

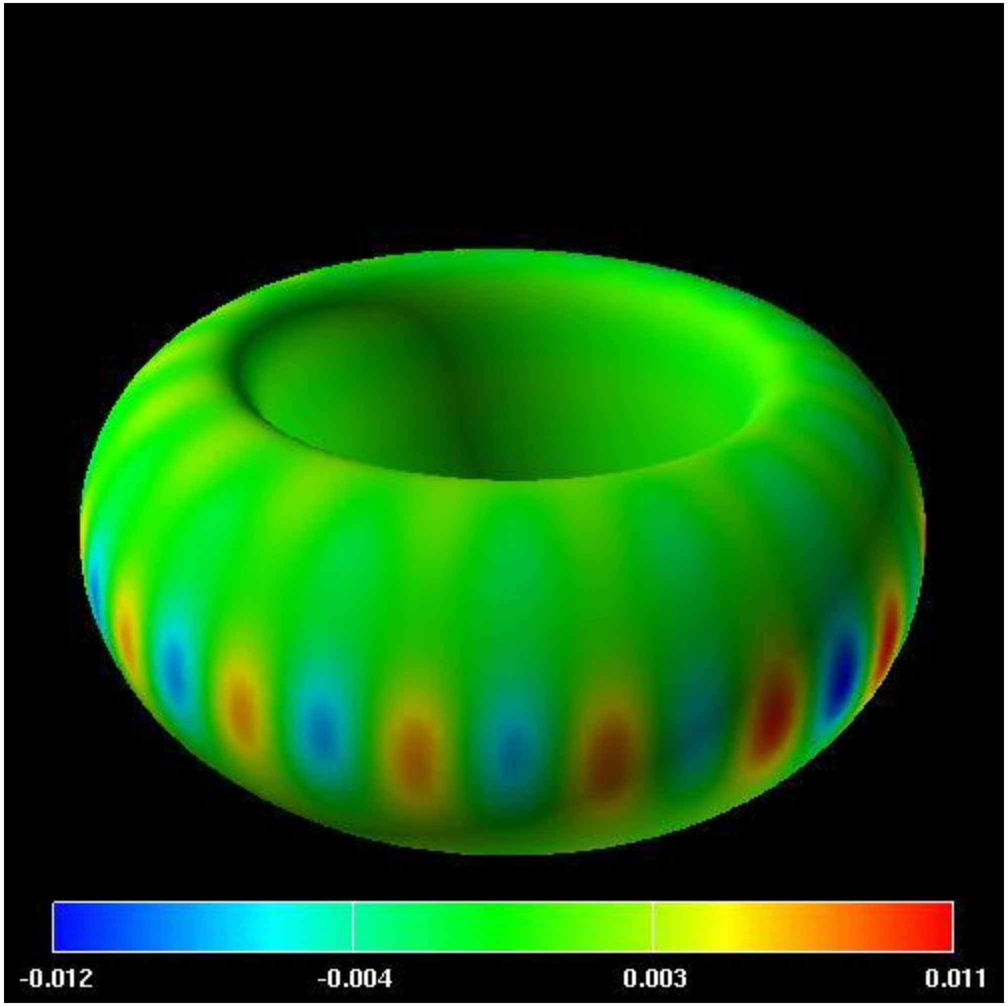

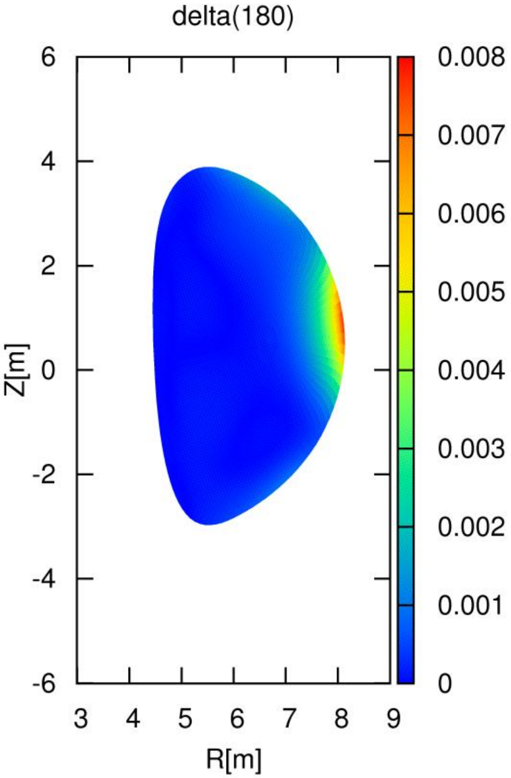

Summary

- The sterallator is a platform to explorer 3D physics.
- 3D MHD equilibrium response is studied in stellarator.
- The stochastization is naturally caused by 3D configuration. => 3D equilibrium responses
- Coupling MHD instability and 3D magnetic field are discussed.
- MHD modeling of CDC event is discussed.
- Applications of 3D tools to tokamaks are shown.